Pergamon

S0306-4522(96)00022-X

THE SUBTHALAMIC NUCLEUS AND THE EXTERNAL PALLIDUM: TWO TIGHTLY INTERCONNECTED STRUCTURES THAT CONTROL THE OUTPUT OF THE BASAL GANGLIA IN THE MONKEY

E. SHINK,* M. D. BEVAN,† J. P. BOLAM† and Y. SMITH*‡

*Centre de Recherche en Neurobiologie, Hôpital de l'Enfant-Jésus and Université Laval, Québec, Canada
†MRC Anatomical Neuropharmacology Unit, and University Department of Pharmacology, Mansfield Road, Oxford OX1 3TH, U.K.

Abstract—The aim of the present study was to elucidate the organization of the interconnections between the subthalamic nucleus and the two segments of the globus pallidus in squirrel monkeys. By making small deposits of tracers in the two segments of the globus pallidus, we demonstrate that interconnected neurons of the subthalamic nucleus and the external pallidum innervate, via axon collaterals, the same population of neurons in the internal pallidum. Furthermore, this organizational principle holds true for different functional regions of the pallidum and the subthalamic nucleus.

Injections of biotinylated dextran amine were made in the dorsal (associative), ventrolateral (sensorimotor) and rostromedial (limbic) regions of the internal pallidum. Following these injections, there were rich clusters of labelled terminals in register with retrogradely labelled perikarya in related functional regions of the subthalamic nucleus and the external pallidum. At the electron microscopic level, the majority of labelled terminals in the external pallidum displayed the ultrastructural features of boutons from the subthalamic nucleus and were non-immunoreactive for GABA, whereas those in the subthalamic nucleus resembled terminals from the external pallidum and displayed GABA immunoreactivity. In both cases, the synaptic targets of the labelled terminals included labelled neurons. These observations suggest that the biotinylated dextran amine injected in the internal globus pallidus was transported retrogradely to perikarya in the external pallidum and the subthalamic nucleus and then anterogradely, via axon collaterals, to the subthalamic nucleus and the external pallidum respectively. This suggestion was supported by injections of biotinylated dextran amine or *Phaseolus vulgaris*-leucoagglutinin in regions of the external pallidum that corresponded to those containing retrogradely labelled cells following injections in the internal pallidum. The clusters of labelled cells and varicosities that resulted from these injections were found in regions of the subthalamic nucleus similar to those labelled following injections in the internal globus pallidus. Furthermore, terminals from the external pallidum and the subthalamic nucleus converged on the same regions in the internal globus pallidus.

The results of the present tracing study define the basic network underlying the interconnections between the external segment of the globus pallidus and the subthalamic nucleus, and their connections with the output neurons of the basal ganglia in primates. Copyright © 1996 IBRO. Published by Elsevier Science Ltd.

Key words: basal ganglia, pallidum, pallidosubthalamic pathway, subthalamopallidal pathway, tract-tracing method, post-embedding immunocytochemistry.

On the basis of electrophysiological and anatomical data, models of the functional organization within the basal ganglia thalamocortical circuit have been suggested.[2,5] These models state that the striatal output reaches the internal pallidum (GPi) via two

‡To whom correspondence should be addressed at: Centre de Recherche en Neurobiologie, Hôpital de l'Enfant-Jésus, 1401, 18ième Rue, Québec, Canada G1J 1Z4.
Abbreviations: ABC, avidin–biotin–peroxidase complex; BDA, biotinylated dextran amine; BSA, bovine serum albumin; d, dendritic shaft; d/BDA, BDA-labelled dendrite; DAB, 3,3'-diaminobenzidine tetrahydrochloride; GPe, external pallidum; GPi, internal pallidum; IC, internal capsule; PB, phosphate buffer; PBS, phosphate-buffered saline; PHA-L, *Phaseolus vulgaris*-leucoagglutinin; PU, putamen; STN, subthalamic nucleus; TBS, Tris-buffered saline.

different pathways, a "direct" inhibitory projection from the striatum to the GPi, and an "indirect" pathway, which involves a GABAergic projection from the striatum to the external pallidum (GPe), an inhibitory projection from the GPe to the subthalamic nucleus (STN) and an excitatory projection from the STN to the GPi. Recent anatomical data revealed the existence of another branch of the indirect pathway which includes a direct projection from GPe to GPi.[8,30,34,39,40,64,67,68,71] According to these models,[2,5] the output of the basal ganglia is under the control of inhibitory and excitatory influences arising from the direct and the indirect pathways, respectively. By virtue of their polarities, activation of the direct pathway facilitates movement by disinhibition of thalamocortical neurons, whereas activation of the

indirect pathway inhibits movements by increasing the inhibition of thalamocortical cells.[2,5,14] A balance between the activity of the two pathways is thus essential for the normal control of motor activities.[14]

However, the exact mechanism by which the direct and indirect striatal afferents to GPi interact to control motor behaviour is poorly understood. The anatomical organization of the direct striatal output to GPi has been thoroughly studied in various species and appears to be highly specific.[12,23,28,77] However, the organization of the indirect pathway is still obscure. The major reason for this is the small size and the heterogeneous functional organization of the STN.[47,75] The combination of these two features complicates the interpretation of data obtained after injections of anterograde tracers in the STN.[11,29,45,62] In these anterograde tracing studies, the injections of tracers resulted in a diffuse and largely unspecific labelling of terminals that extended throughout the entire extent of the pallidal complex in primates. On the basis of these findings, the STN was considered as a source of non-specific excitatory influences on the globus pallidus.[43,48] Another possible interpretation of these data is that, in fact, the projection is highly specific but the injections involved neighbouring neuronal groups that projected to different regions of the globus pallidus. The relative size of the injection sites in the STN compared to the size of the STN itself makes this possibility very likely.[29,45,62] Other investigators addressed this issue by means of retrograde transport from the globus pallidus to the STN,[11,16,49] but in these cases the injection sites covered large areas of the GPe and GPi. We have therefore re-examined the organization of the interconnections between the two segments of the globus pallidus and the STN in primates. Since recent studies have emphasized the importance of the projection from the GPe (or globus pallidus in non-primates) to the GPi (or entopeduncular nucleus in non-primates),[7,8,30,34,67,68] one of the aims of the present study was to examine the location of neurons in the STN that innervate these interconnected regions. This was achieved by placing iontophoretic deposits of biotinylated dextran amine (BDA)[9,52,72] in interconnected regions of the GPi and GPe.

The results of this study have been presented in abstracts.[65,66]

EXPERIMENTAL PROCEDURES

Six adult male squirrel monkeys (*Saimiri sciureus*) were used in the present study. Each animal was anaesthetized with a mixture of ketamine hydrochloride (Ketaset, 70 mg/kg, i.m.) and xylazine (10 mg/kg, i.m.) before being fixed in a stereotaxic frame. The depth of anaesthesia was determined by monitoring heart-rate, respiration rate, muscle tone, as well as corneal and toe-pinch reflexes. The surgical and anaesthesia procedures were performed according to the guidelines of the Canadian Council on Animal Care. In four animals, BDA was injected bilaterally in different regions of the pallidal complex, while in another animal, a unilateral injection of BDA was performed in GPi. In the last animal, BDA was injected in both pallidal segments on one side of the brain and *Phaseolus vulgaris*-leucoagglutinin (PHA-L) was delivered in GPe on the other side. The stereotaxic coordinates were derived from the atlas of Emmers and Akert.[17] The two tracers were injected iontophoretically using the same parameters. The BDA (Molecular Probes, Eugene, OR, U.S.A.; 5% in distilled water) and PHA-L (2.5% solution in phosphate buffer, 0.01 M, pH 8.0) were loaded in glass micropipettes (tip diameter 20–30 μm) and delivered with a 7-μA positive current for 20 min by a 7 s on/7 s off cycle.[24] For the first two days after the surgery, the animals received injections of analgesic (buprenorphine; 0.01 mg/kg, i.m.) twice daily.

After seven to 10 days, the animals were deeply anaesthetized with an overdose of pentobarbital and perfuse-fixed with 500–700 ml of cold oxygenated Ringer solution followed by 1.2 l of fixative containing 3% paraformaldehyde and 0.5% glutaraldehyde in phosphate buffer (PB; 0.1 M, pH 7.4). The unbound aldehydes were then washed out by perfusing with 1 l of cold PB (0.1 M, pH 7.4). After perfusion, the brains were dissected out from the skull, cut in 10-mm-thick blocks in the transverse plane and stored in phosphate-buffered saline (PBS, 0.01 M, pH 7.4) until sectioning. The blocks were then cut in 60-μm-thick transverse sections with a vibrating microtome, collected in cold PBS and treated for 20 min with sodium borohydride (1% in PBS). The sections were repeatedly washed in PBS and processed to reveal the tracers according to protocols suitable for light and electron microscopy.

Histochemical localization of biotinylated dextran amine

Light microscopy. A series of sections was washed in PBS and processed to reveal the transported BDA. They were placed in an avidin–biotin–peroxidase solution (ABC; Vector Laboratories, Burlingame CA, U.S.A.; 1:100 in PBS including 1% bovine serum albumin (BSA) and 0.3% Triton X-100) for 12–16 h at room temperature. They were then washed in PBS and Tris buffer (0.05 M, pH 7.6) before being placed in a solution containing 3,3′-diaminobenzidine tetrahydrochloride (DAB, 0.025%; Sigma Chemicals, St Louis, MI, U.S.A.), 0.01 M imidazole (Fisher Scientific, Nepean, Ontario, Canada) and 0.006% hydrogen peroxide for 10–15 min. The reaction was stopped by repeated washes in PBS. The sections were then mounted on to gelatin-coated

Fig. 1. Labelling in STN and GPe or GPi after BDA injections in the associative territory of GPi and GPe, respectively. (A,C,E) Photomicrographs depicting the labelling in STN (C) and GPe (arrows in E) that resulted from an injection of BDA in the dorsomedial part of GPi (A). The relationships between BDA-containing varicosities and retrogradely labelled cells as well as unlabelled perikarya in the cluster of labelling in STN are shown at higher magnification in Fig. 9A,B. (B,D,F) Labelling in STN (D) and GPi (arrow in F) resulting from an injection of BDA in a region of GPe (B) that roughly corresponds to that containing the most lateral cluster of labelled cells after the GPi injection (compare B and E). The morphological features of the terminals that form the band of labelling in GPi are shown at higher magnification in Fig. 11A,B. The rostrocaudal levels of the sections are indicated in the upper right corner of the micrographs. IC, internal capsule; Pu, putamen. Scale bars = 1 mm (A, also applies to B); 1 mm (C, also applies to D); 0.5 mm (E, also applies to F).
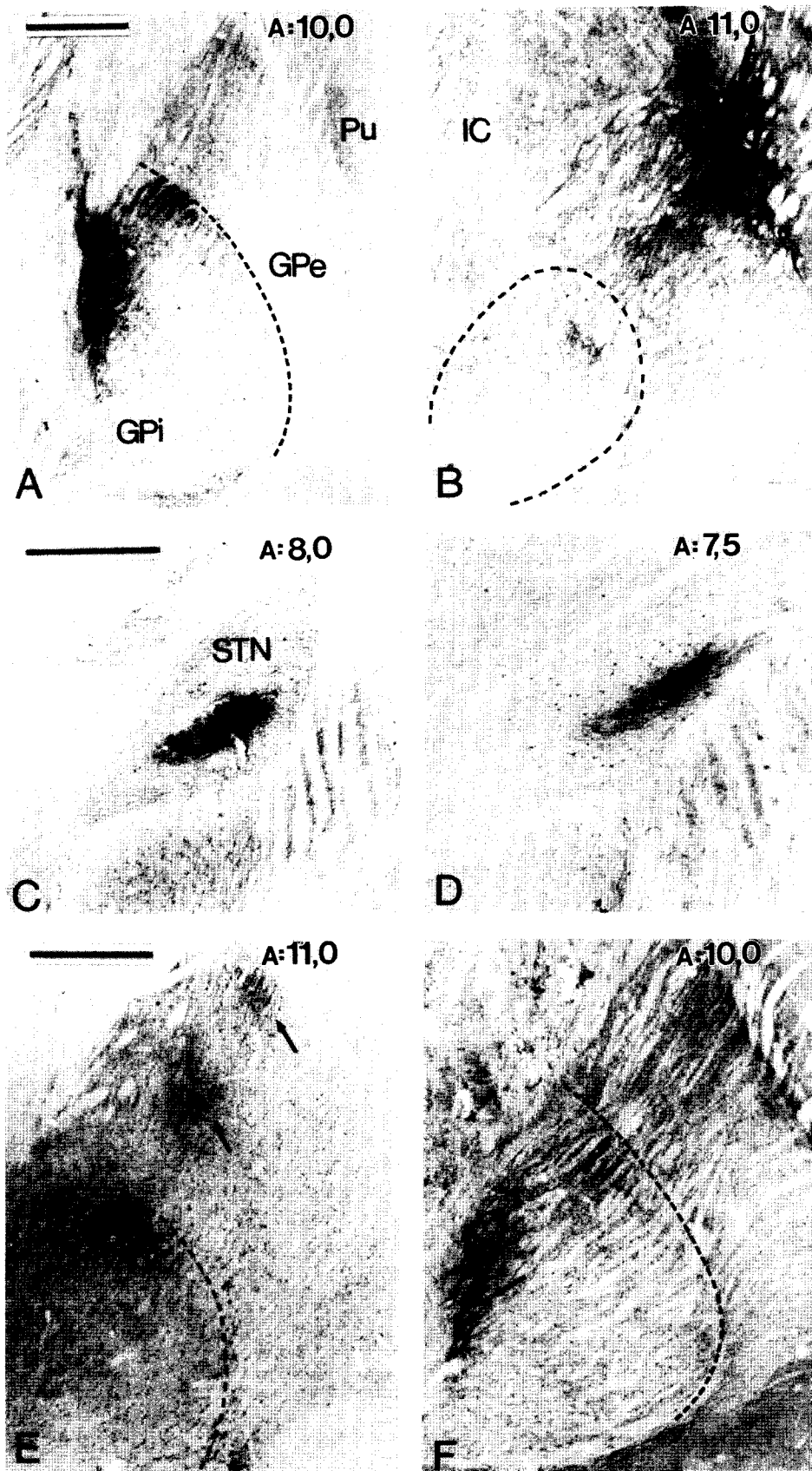
Fig. 1.

slides, dehydrated and a coverslip was applied with Permount.

Electron microscopy. A series of sections including the pallidal complex or the STN were processed for the localization of the transported BDA in the electron microscope. The sections were placed in a cryoprotectant solution (PB, 0.05 M, pH 7.4, containing 25% sucrose and 10% glycerol) for 20–30 min. After having sunk, they were frozen at −80 C for 20 min. They were then thawed and washed many times in PBS before being processed to localize BDA according to the protocol described above, except that no Triton X-100 was added to the ABC solution and the incubation was carried out at 4°C for 48 h. Once the BDA was localized, the sections were washed in PB (0.1 M, pH 7.4), postfixed in osmium tetroxide (1% in PB; 0.1 M, pH 7.4) for 20–30 min, and dehydrated in a graded series of alcohols and propylene oxide. Uranyl acetate was added to the 70% ethanol (40 min) to improve the contrast in the electron microscope. The sections were then embedded in resin (Durcupan ACM, Fluka) on microscope slides and cured for 48 h at 60 C.

Immunohistochemical localization of Phaseolus vulgaris-leucoagglutinin

The sections including the PHA-L injection site in GPe as well as a series of sections containing GPi and STN were prepared for the localization of PHA-L in the light microscope. They were first incubated with a goat anti-PHA-L antiserum (Vector Labs; 1:2000 in PBS containing 0.3% Triton X-100 and 1% normal rabbit serum) for 16 h. This was followed by an incubation with biotinylated rabbit anti-goat IgG (Vector Labs; 1:200 in PBS/0.3% Triton X-100/1% normal rabbit serum) for 2 h and then an incubation in ABC (1:100 in PBS/0.3% Triton X-100/1% BSA) for two additional hours. The incubations were all carried out at room temperature. The peroxidase bound to PHA-L was revealed with DAB (see above). Once the reaction was completed, the sections were mounted on to gelatin-coated slides, dehydrated and a coverslip was applied with Permount.

Analysis of the material

The sections containing the injection sites were examined with a Nikon light microscope equipped with a camera lucida to determine the extent of the tracers in their respective targets.

The sections of GPe and STN prepared for electron microscopy were chosen from the case illustrated in Fig. 6, whereas the sections selected in GPi were taken from the case illustrated in Fig. 5. Once located, regions that contained rich plexuses of BDA-positive terminals were cut out from the slides and glued to the top of resin blocks with cyanoacrylate glue. Serial ultrathin sections were then cut on an ultramicrotome (Reichert–Jung Ultracut E), collected on Pioloform-coated single-slot gold or copper grids, stained with lead citrate[54] and examined in an electron microscope (Philips EM300; Philips CM10). The sections were randomly scanned for the presence of labelled boutons that formed synaptic contacts. The number and the ultrastructural features of BDA-positive terminals encountered were

recorded. The size of the various types of terminals was measured from electron micrographs with the softwares Ultimage and MacStereology prepared for Macintosh computers.

Post-embedding immunocytochemistry for GABA

A series of sections including the STN or GPe were processed for post-embedding immunocytochemistry for GABA. The post-embedding immunogold procedure was carried out with an antiserum raised in rabbit against GABA. The production, characterization and specificity of this antiserum have been described in detail elsewhere.[31,69,70] The protocol for immunostaining was that introduced by Somogyi and Hodgson[69] including recent modifications.[51] Briefly, a series of adjacent ultrathin sections was preincubated for 10 min in Tris-buffered saline (TBS; 0.05 M, pH 7.6) containing 0.01% Triton X-100. This was followed by an overnight incubation at room temperature with the primary antiserum (1:5000 dilution) diluted in TBS/0.01% Triton X-100. The sections were then washed three times (2 × 10 min and 1 × 30 min) in TBS/0.01% Triton X-100 followed by TBS (0.05 M, pH 8.2) for 10 min. They were then incubated with the gold-conjugated goat anti-rabbit IgG (BioCell; 1:25 in TBS 0.05 M, pH 8.2) for 90 min at room temperature, washed in distilled water and stained with uranyl acetate (1% in distilled water) for 90 min. Finally, after having been washed in distilled water and stained with lead citrate,[54] they were examined with a Philips EM 300 electron microscope.

Control experiments

The specificity of labelling was tested by incubation with solutions in which the primary antiserum was replaced with non-immune rabbit serum. After such incubation, the tissue was devoid of gold particles indicating that the GABA immunolabelling was due to the primary antibodies. Another series of control grids was incubated with GABA antiserum that had undergone liquid-phase pre-adsorption with structurally related amino acids conjugated to ethanolamine with glutaraldehyde.[13] Each antiserum was preadsorbed against taurine, GABA, glutamate and glutamine conjugates. After such incubation, the tissue was almost completely devoid of gold particles in the cases where the GABA antiserum was pre-adsorbed with GABA–glutaraldehyde conjugates, whereas pre-adsorption of the antiserum with other amino acids conjugates had no effect on the intensity of staining. These control experiments indicate that the GABA immunostaining described in the present study is specific.

RESULTS

Location of injection sites

In order to analyse the interconnections between the GPe, STN and GPi, the following approaches were used. Firstly, we injected BDA in different regions of the GPi. Secondly, we determined the location of the retrogradely labelled cells in the GPe

Fig. 2. Labelling in STN after BDA injections in the sensorimotor territory of GPi and GPe. (A,C,E) Photomicrographs showing the labelling in STN (C) and GPe (arrow in E) after injection of BDA in the ventrolateral part of GPi (A). The relationships between the labelled terminals and the retrogradely labelled cells in the cluster of labelling in GPe are depicted at higher magnification in Fig. 10A,B. (B,D,F) Labelling in STN resulting from an injection of BDA in a region of GPe (B) that roughly corresponds to that containing the retrogradely labelled cells after injection in GPi (compare B and E). Note the clear demarcation between the cluster of labelling in STN and the rest of the unstained neuropil (F). The anteroposterior coordinates for each section are indicated in the upper right corner of the micrographs. Abbreviations as in Fig. 1. Scale bars = 1 mm (A); 0.5 mm (B, also applies to E); 1 mm (C, also applies to D); 0.25 mm (F).
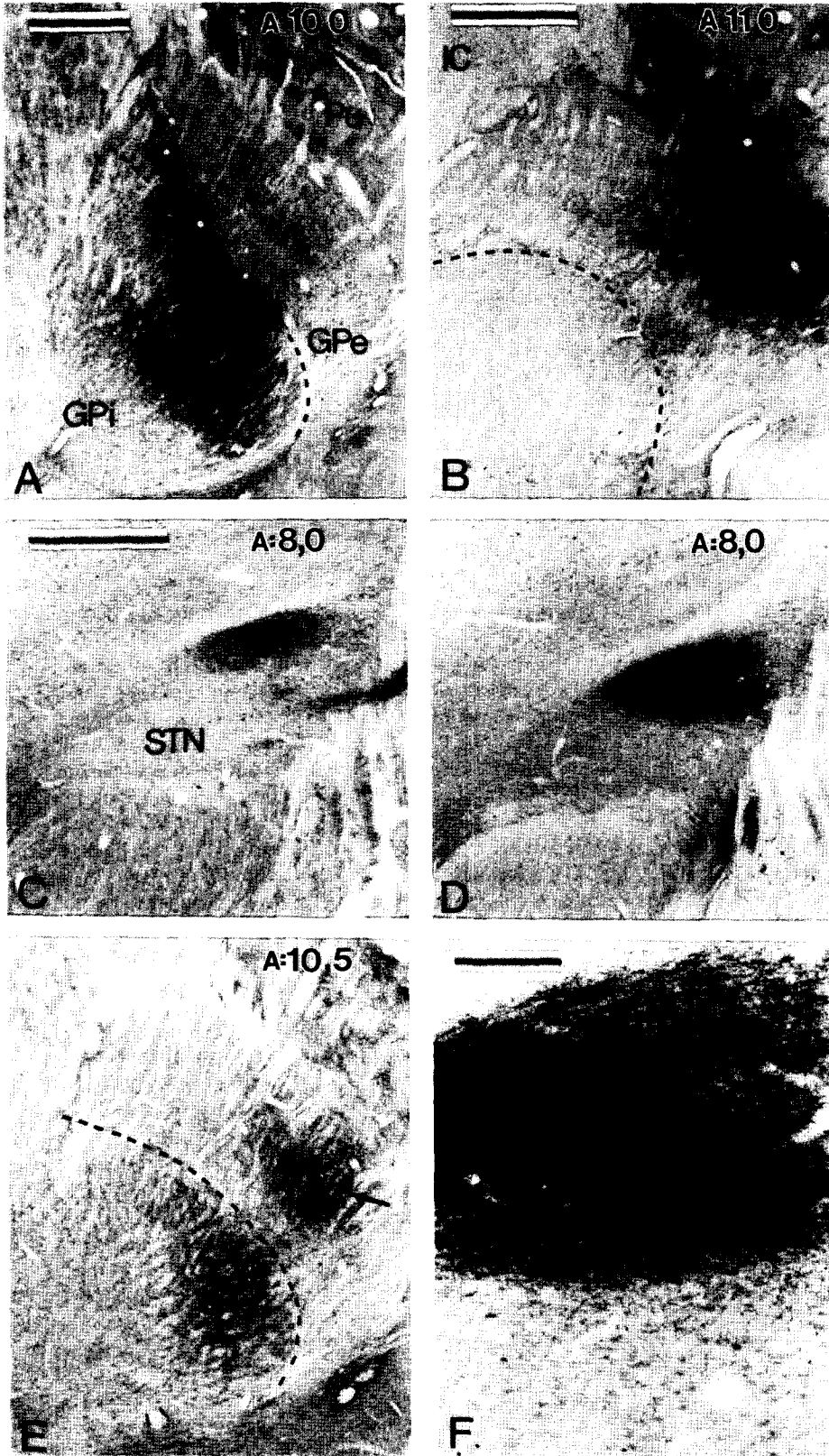
Fig. 2.

following these injections. Thirdly, we delivered BDA or PHA-L in those regions of the GPe that were found to contain retrogradely labelled cells. Using this approach, we succeeded in injecting interconnected pools of neurons in the dorsal third (1 in GPi, 2 in GPe) (Figs 1, 3, 4) and the ventrolateral region (2 in GPi, 3 in GPe) (Figs 2, 5, 6, 7) of the GPi and GPe. In another case, BDA was injected in the ventromedial part of the GPi, without injection in the corresponding region of the GPe (Fig. 8). Most of the animals received injections of BDA, except in one case where PHA-L was delivered in the ventral part of the GPe (Fig. 7). In general, the injections were confined to their respective targets except for a slight contamination of the dorsal part of the pallidum after injections in the ventral GPi (Figs 2A, 5E, 8D). In the cases that received injections of BDA in the dorsal third of the GPe, the injection sites damaged the medullary laminae (Figs 1B, 4C).

Pattern of labelling following deposits of tracers in the internal and external pallidum

Each of the injections in either the GPi or the GPe resulted in a similar pattern of labelling in the corresponding division of the pallidal complex and the STN.

Deposits of tracer in the GPi led to the labelling of dense clusters of axons and axonal varicosities that were largely in register with labelled neurons in both the GPe and the STN (Figs 1A,C,E, 2A,C,E, 9A,B, 10A,B). Only a few of the labelled neurons were found outside the region of axon labelling. In both structures the labelled cells were often stained in a Golgi-like manner and were interspersed with unlabelled neurons (Figs 9A,B, 10A,B). The perikarya and proximal dendrites of the labelled and unlabelled neurons were often closely apposed by the labelled axonal varicosities (Figs 9A,B, 10B).

The injections of tracers in the GPe resulted in the labelling of dense clusters of axons and axonal varicosities in both the STN and the GPi (Figs 1B,D, 2B,D). In the STN, the axonal labelling was largely in register with a population of labelled neurons (Fig. 2D). As was the case following the injections in the GPi, the perikarya and proximal dendrites of labelled and unlabelled neurons in the STN were closely apposed by the labelled terminals. No labelled neurons were observed in the GPi. However, at least two populations of axonal boutons characterized on morphological grounds were identified (Fig. 11A,B).

Correspondence and topography of labelling in the subthalamic nucleus after biotinylated dextran amine injections in interconnected regions of the internal and external pallidum

The injection sites in the GPi or GPe and the subsequent labelling in the pallidum and the STN are illustrated schematically in Figs 3–8. After BDA injections confined to the dorsal third of the GPi (Figs 1A, 3E), a cluster of labelling was found in the

central part of the STN (Figs 1C, 3G–J). Apart from a few scattered perikarya, the labelled varicosities and cell bodies were in complete register at different rostrocaudal levels of the STN (Fig. 3G–J). These injections in the dorsal GPi also resulted in two clusters of labelled varicosities in register with retrogradely labelled cells that were confined to the dorsal third of the GPe (Figs 1E, 3C,D). The labelling was predominantly in sectors of the GPe located 0.5–1.0 mm more rostral than the injection site. The rostral and caudal poles of the GPe were devoid of labelling (Fig. 3A,F).

Injections of BDA into the sector of the GPe where neurons were labelled after injections in the dorsal third of the GPi (compare Figs 1B and 1E, 3C and 4C) led to dense aggregates of labelling in the STN and the GPi. In the STN, clusters of labelled varicosities were in register with labelled perikarya and were confined to the sector of the nucleus that was labelled after the BDA injection in the GPi (compare Figs 1C and 1D; 3H,I and 4H,I), except that there was a slight lateral shift. More labelled cells were found outside the main cluster of labelling after this injection than after injections in the GPi (Figs 1C,D, 3G–J, 4G–J). The injection in the GPe also led to a dense cluster of labelling in the GPi (Figs 1F, 4E) that was located precisely where the BDA injection site was in the preceding case (compare Figs 1A and 1F, 3E and 4E).

In another case (not shown), the BDA injection was larger and more medial in the dorsal part of the GPe and involved the internal medullary lamina. The pattern and location of labelling in the STN corresponded to that described for the preceding case (Fig. 4G–J), except that the labelled structures were slightly shifted ventromedially. In the GPi, the pattern of labelling was similar to that obtained after the lateral injection (Figs 1F, 4E).

The BDA injections confined to the ventrolateral two-thirds of the GPi (Figs 2A, 5E) led to dense aggregates of labelling in the dorsolateral region of the STN, but excluding the lateralmost part of the nucleus (Figs 2C, 5G–J). The majority of labelled cells in the STN were in register with the labelled varicosities although a few were located more ventrally (Figs 2C, 5H,I). In the GPe, a dense cluster of labelled cells and varicosities was confined to the central part of the structure (Figs 2E, 5C,D). Like the injections in the dorsal third of the GPi, the densest zones of staining in the GPe were 0.5–1.0 mm more rostral than the injection site in the GPi (Fig. 5C,D).

An injection of BDA confined to the ventral region of the GPe that contained retrogradely labelled cells after BDA injection in the ventrolateral GPi (compare Figs 2B and 2E, 5C and 6C) led to a cluster of labelling in the dorsolateral STN (Figs 2D,F, 6G,I). This labelling was in the same region of the STN that was labelled after tracer injections in the ventrolateral GPi (compare Figs 2C and 2D, 5H,I and 6H,I), except that the rostrolateral pole contained labelled elements after injection in the GPe but not after that

A (A 12,5)   **B** (A 11,5)   **C** (A 11,0)

D (A 10,5)   **E** (A 10,0)   **F** (A 9,0)

G (A 8,5)   **H** (A 8,0)   **I** (A 7,5)   **J** (A 7,0)
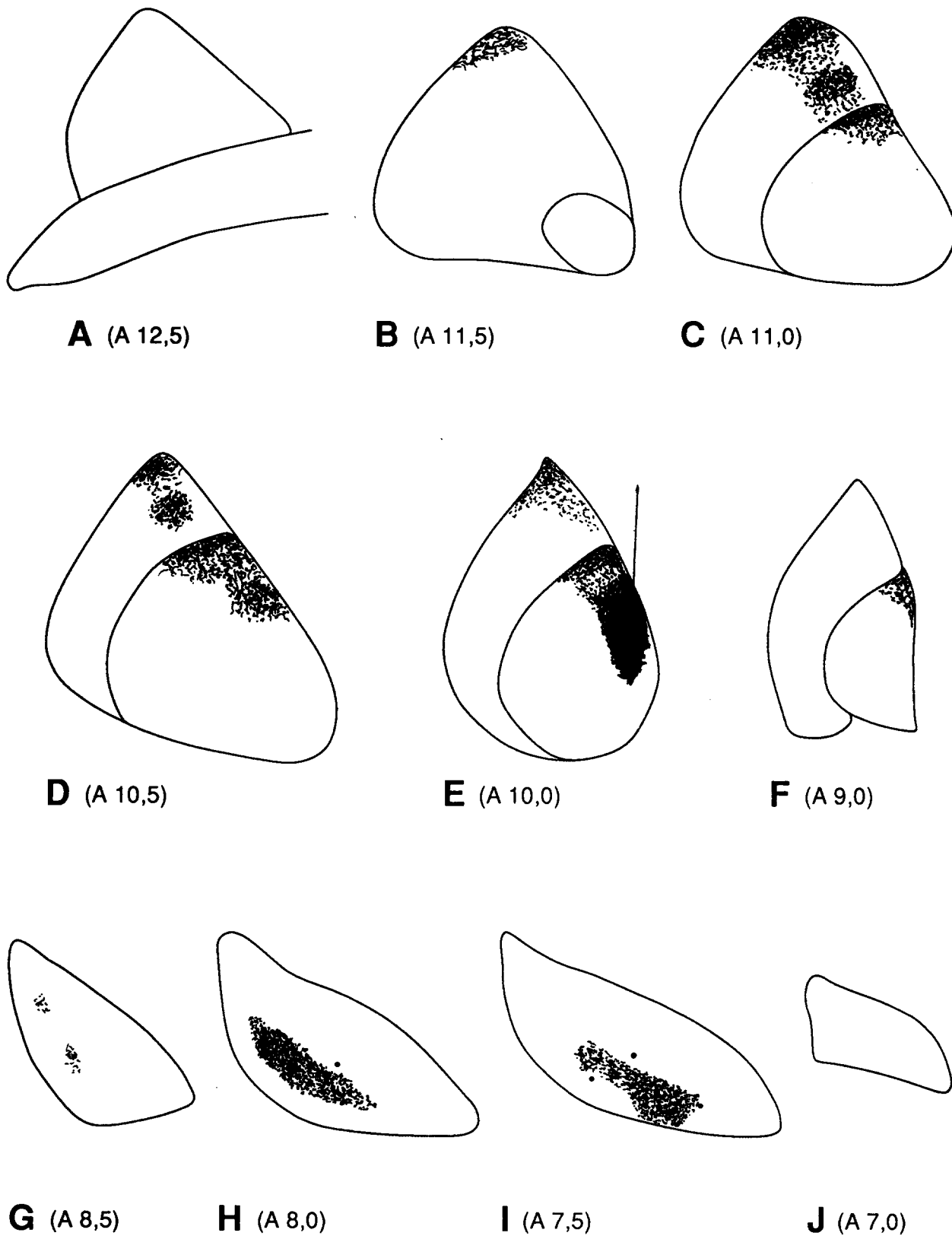
Fig. 3. Schematic drawing through the globus pallidus (A–F) and the STN (G–J) of the squirrel monkey to illustrate the distribution of labelled fibres (sinuous lines), terminals (small black dots) and perikarya (red dots) after BDA injection in the dorsal third of GPi (E). One red dot indicates three retrogradely labelled cells. Note the close overlap between the retrogradely labelled cells and the labelled fibres and terminals in GPe and STN. The anteroposterior coordinates are indicated in parentheses for each drawing.

A (A 12,5)   **B** (A 11,5)   **C** (A 11,0)

D (A 10,5)   **E** (A 10,0)   **F** (A 9,0)
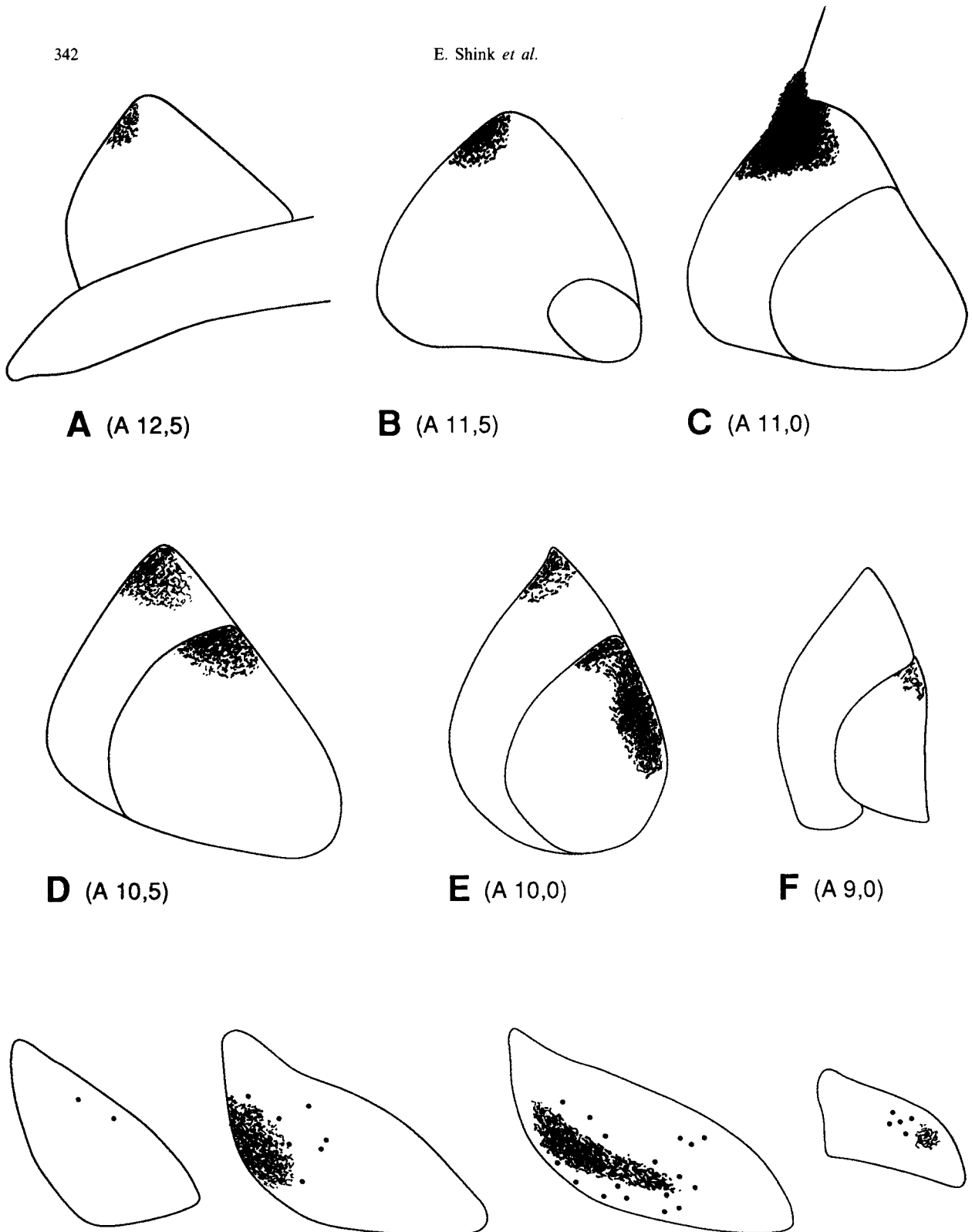
Fig. 4. Schematic drawing through the globus pallidus (A–F) and the STN (G–J) of the squirrel monkey
to illustrate the distribution of labelled fibres (sinuous lines), terminals (small black dots) and perikarya
(red dots) after BDA injection in the dorsal third of GPe (C). One red dot indicates three retrogradely
labelled cells. Note that the location of the injection site corresponds to that where the retrogradely labelled
cells were found after injections in the dorsal part of GPi (see Fig. 3). The anteroposterior coordinates
are indicated in parentheses for each drawing.

A (A 12,5)   **B** (A 11,5)   **C** (A 11,0)

D (A 10,5)   **E** (A 10,0)   **F** (A 9,0)
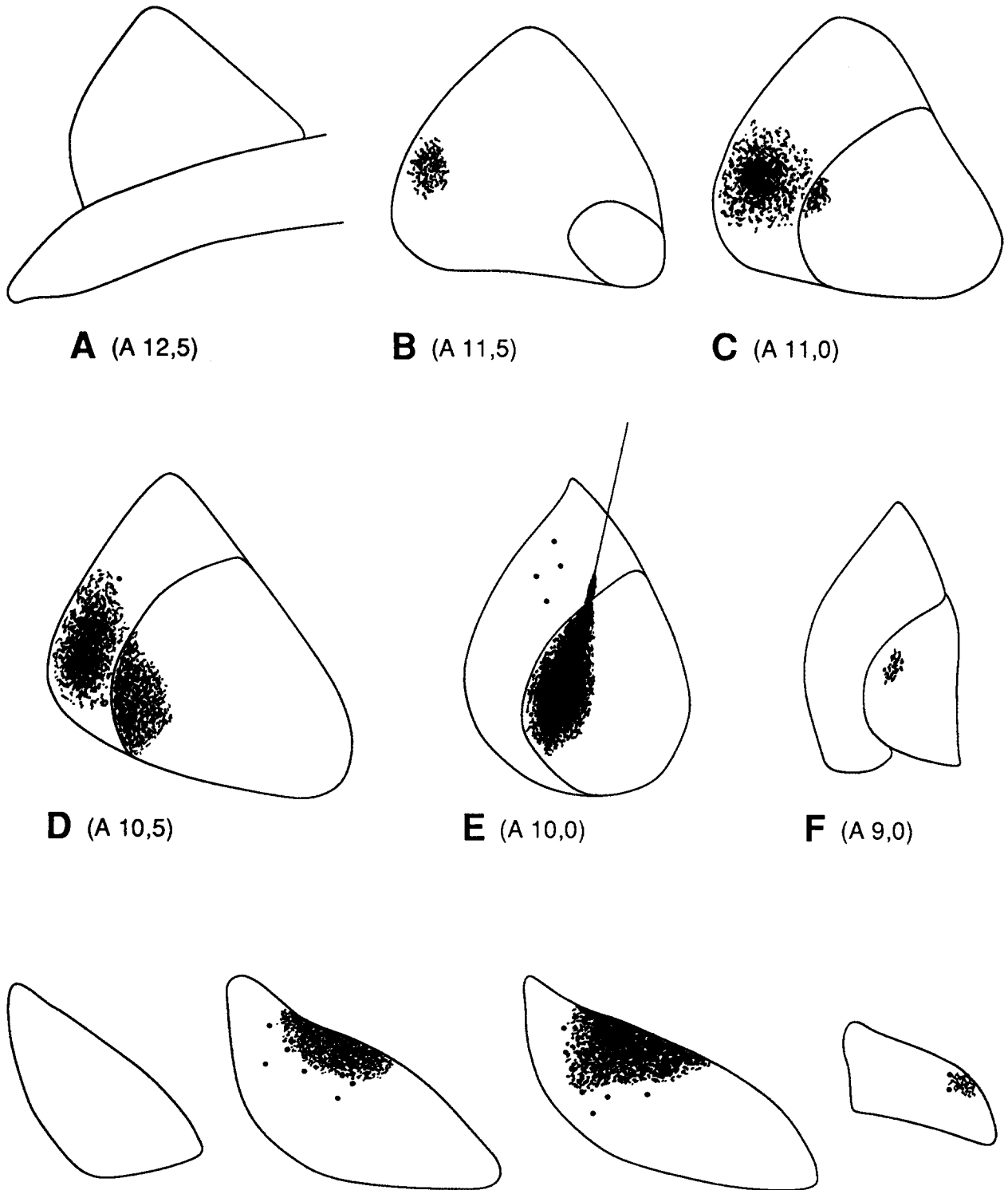
Fig. 5. Schematic drawing through the globus pallidus (A–F) and the STN (G–J) of the squirrel monkey to illustrate the distribution of labelled fibres (sinuous lines), terminals (small black dots) and perikarya (red dots) after BDA injection in the ventrolateral two-thirds of GPi (E). One red dot indicates three retrogradely labelled cells. The anteroposterior coordinates are indicated in parentheses for each drawing.

A (A 12,5)   **B** (A 11,5)   **C** (A 11,0)

D (A 10,5)   **E** (A 10,0)   **F** (A 9,0)

G (A 8,5)   **H** (A 8,0)   **I** (A 7,5)   **J** (A 7,0)
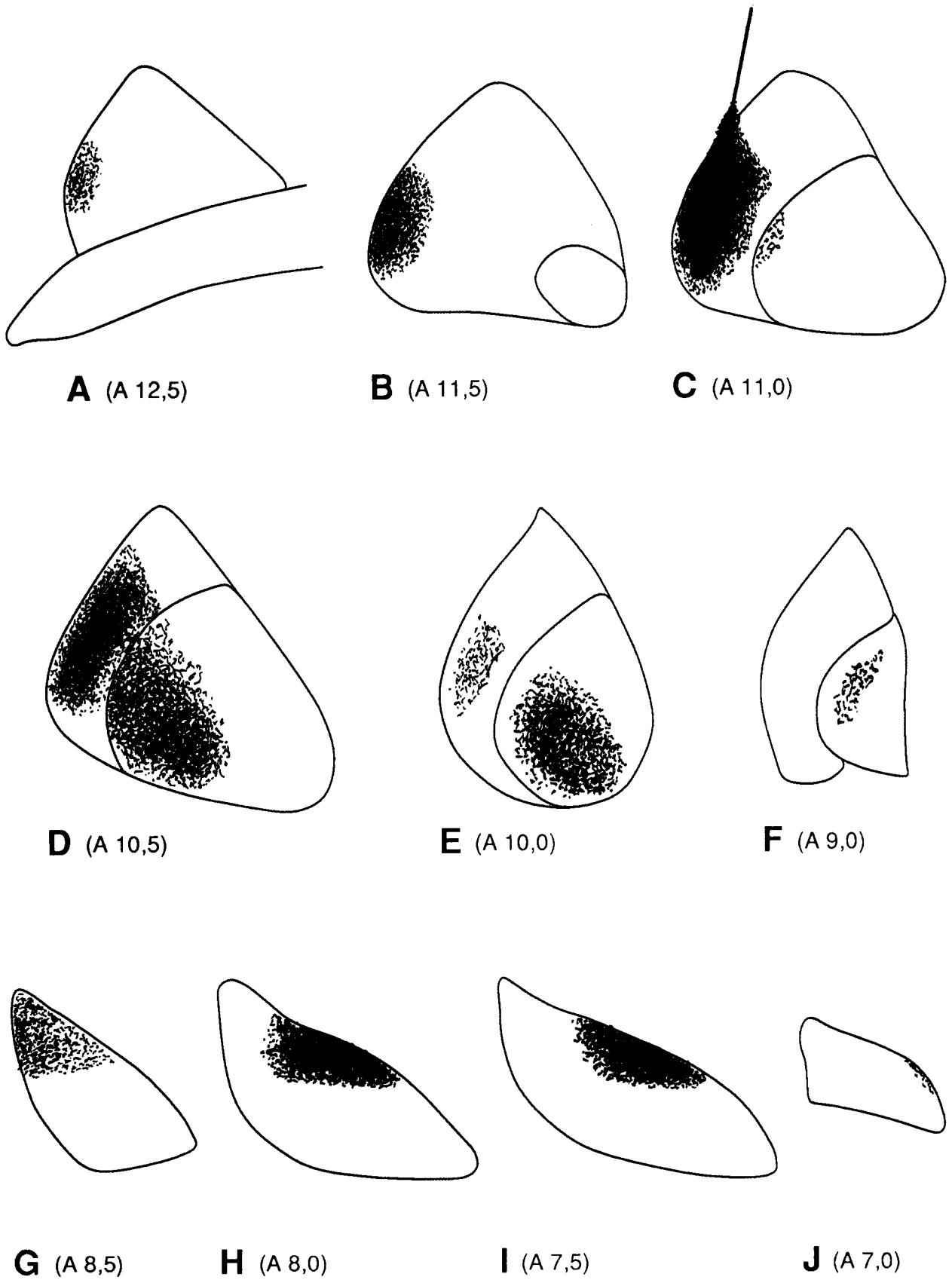
Fig. 6.

in the GPi (compare Figs 5G and 6G). None of the retrogradely labelled cells were outside the cluster of labelled varicosities following the injection in the GPe (Figs 2D,F, 6G–J). A rich cluster of labelled varicosities occurred in the region of the GPi where the injection of BDA was made in the preceding case (compare Figs 5E and 6E) except that the labelling extended slightly more in the rostrocaudal and mediolateral planes. Similar patterns of labelling occurred following PHA-L injections in the same regions of the GPe (compare Figs 6C and 7C) except that the labelling was not as extensive in the GPi (compare Figs 6 and 7).

In the single case that received an injection of BDA confined to the ventromedial region of the GPi (Fig. 8), a dense cluster of labelling was found in the dorsomedial part of the STN (Fig. 8G–I). In contrast to injections in the more lateral part, the injection located more medially in the GPi led to labelling in the rostral pole of the STN that was generally placed more medially (compare Figs 5H,I and 8G–I). In both cases, a few retrogradely labelled cells were found more ventral than the main cluster of labelling (Fig. 8G–I). In the GPe the cluster of labelled axons, varicosities and cells was found in the rostroventral region just caudal to the anterior commissure (Fig. 8B).

Ultrastructural characteristics of labelled terminals in the subthalamic nucleus and external pallidum after injections of biotinylated dextran amine in the internal pallidum

In order to determine the exact source of the labelled boutons in the STN and GPe after BDA injections in the GPi, we analysed their ultrastructural features, determined their pattern of synaptic innervation and tested whether they were immunoreactive for GABA. In the electron microscope, two categories (so-called type 1 and type 2) of BDA-positive terminals were seen in the STN. The type 1 boutons (89%; $n = 475$) were large (2–4 μm in diameter) and contained pleomorphic vesicles as well as numerous mitochondria (Fig. 9D). They formed symmetric synapses with perikarya (31%) and dendritic shafts (69%) of STN neurons (Fig. 9D); some of which (13%) were retrogradely labelled from the deposit of BDA in the GPi. In the GABA-immunolabelled sections, these boutons were identified as GABA-positive by the high density of immunogold particles associated with them (Fig. 9D). Type 2 terminals (11%; $n = 58$) were much rarer, contained round synaptic vesicles and formed asymmetric

synapses with labelled (13.8%) (Fig. 9C) and unlabelled (86.2%) dendrites.

In the GPe, three types of labelled terminals were found. The majority (82%; $n = 460$) displayed the ultrastructural features of type 2 terminals found in the STN and formed asymmetric synapses predominantly with dendritic shafts (98.7%) (Fig. 10D) and rarely with perikarya (1.3%). Twenty per cent of the dendrites, but none of the perikarya, in contact with the type 2 boutons were labelled with BDA. These boutons did not display immunoreactivity for GABA (Fig. 10D). A second type, which accounted for only a small proportion (12%; $n = 67$) of labelled terminals displayed ultrastructural features similar to those of the type 1 boutons (Fig. 9D) and formed symmetric synapses with dendrites (50%) and perikarya (50%). None of the elements in contact with the type 1 boutons were labelled with BDA. A third category of labelled terminals (7%; $n = 39$), referred to as type 3 boutons, contained ovoid synaptic vesicles, formed symmetric synapses with unlabelled dendritic shafts and displayed GABA immunoreactivity (Fig. 10C).

Ultrastructural features of labelled terminals in the internal pallidum after biotinylated dextran amine injections in the external pallidum

In the light microscope, two types of varicosities appeared to compose the clusters of labelling in the GPi after injections in the GPe (Fig. 11A,B). The first category consisted of large-sized boutons (2–4 μm in diameter) that formed pericellular baskets around the perikarya and proximal dendrites of GPi neurons (Fig. 11B). The second class comprised medium-sized varicosities (0.5–2.5 μm in diameter) that were associated preferentially with dendritic shafts (Fig. 11B). In the electron microscope, the three types of labelled boutons described above were found. The type 1 ($n = 47$; 44%; 11D,E) and the type 2 ($n = 53$; 50%; Fig. 11C) terminals accounted for 94% of the 106 labelled terminals that were examined. The remaining terminals ($n = 6$; 6%) displayed the ultrastructural features of the type 3 boutons (Fig. 10C).

DISCUSSION

The neuronal network underlying the interconnections between the GPe and the STN and the relationship of these structures with the GPi has been the subject of many studies.[11,27,29,38,45,47–50,56,57,61,65–68] Elucidation of this network is of critical importance in our understanding of how the "indirect" pathways influence neurons of the GPi and hence the output of the

Fig. 6. Schematic drawing through the globus pallidus (A–F) and the STN (G–J) of the squirrel monkey to illustrate the distribution of labelled fibres (sinuous lines), terminals (small black dots) and perikarya (red dots) after BDA injection in the ventral part of GPe (C). One red dot indicates three retrogradely labelled cells. Note that the location of the injection site corresponds to that where the retrogradely labelled cells were found after injection in the ventrolateral region of GPi (see Fig. 5C). The anteroposterior coordinates are indicated in parentheses for each drawing.

A (A 12,5)

B (A 11,5)

C (A 11,0)

D (A 10,5)

E (A 10,0)

F (A 9,0)

G (A 8,5)   **H** (A 8,0)   **I** (A 7,5)   **J** (A 7,0)
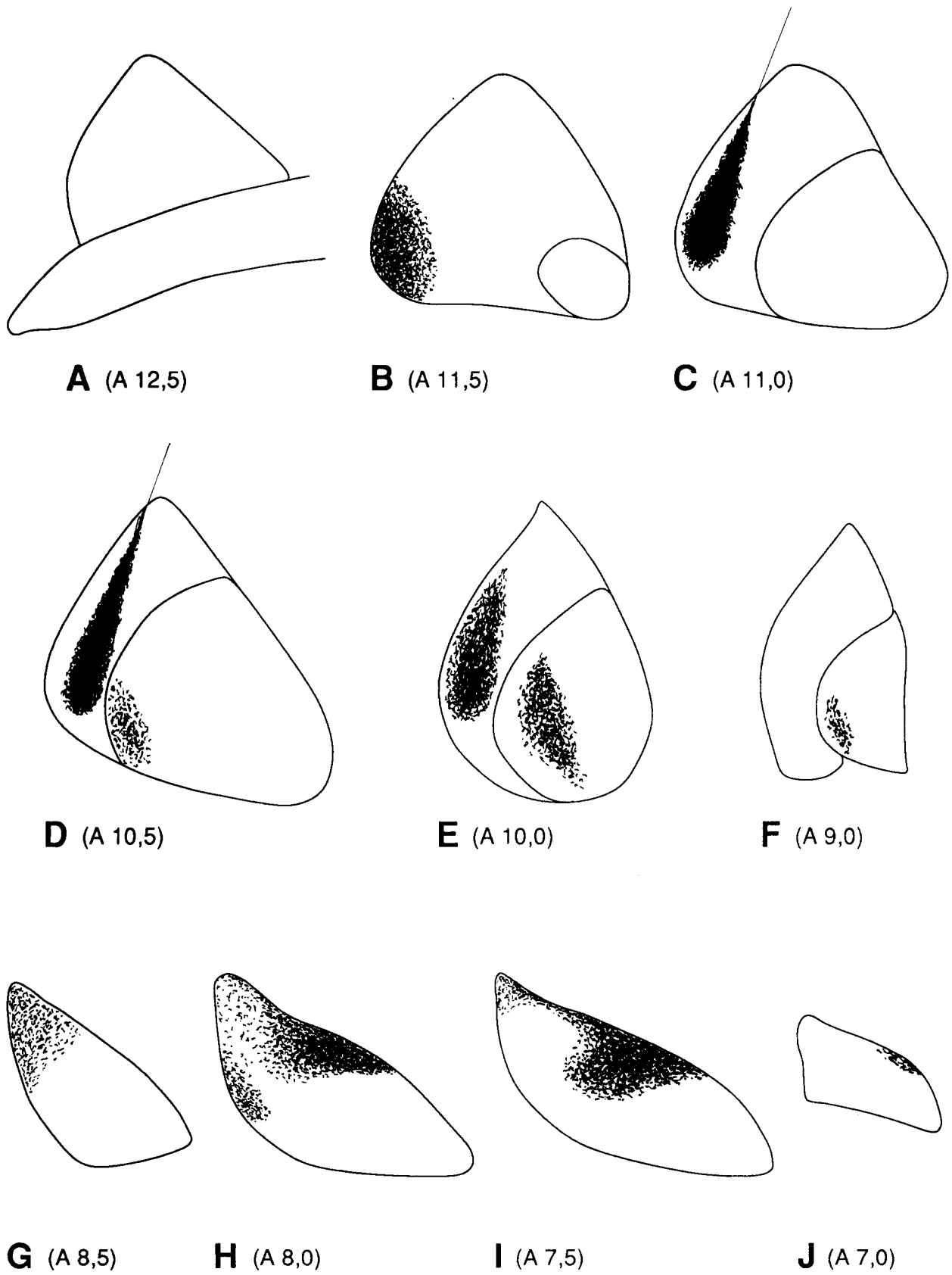
Fig. 7.

basal ganglia. By the use of a tracer that is transported in both retrograde and anterograde fashions we describe the basic circuit underlying these interconnections. The results demonstrate that the interconnections between the two divisions of the pallidal complex and the STN are much more specific than previously suspected.[11,29,45,62] The basic circuit is such that interconnected groups of neurons in the GPe and STN innervate, via axon collaterals, the same population of neurons in the internal pallidum, i.e. output neurons of the basal ganglia. A basic principle that emerged is that the topography of the tight interconnections respects the functional organization of both pallidal segments and the STN (Fig. 13). These findings have important implications for the understanding of the neuronal mechanisms that underlie the roles of the basal ganglia in the control of motor activity in primates.

Interpretation of labelling: possible sources of labelled boutons in the subthalamic nucleus and external pallidum

As mentioned in the introduction, the data obtained so far relating to the organization of the subthalamopallidal projection in primates must be interpreted with caution because of technical problems inherent to the approaches used to investigate this issue. In the present study, these problems were overcome by the use of the neuronal tracer BDA. The fact that BDA can be injected iontophoretically enabled us to deliver relatively small quantities of tracer that were mostly confined to the different functional territories of the GPe and GPi. After injections of BDA in the GPi, dense plexuses of labelled terminals in register with retrogradely labelled perikarya were found in the STN and GPe. The presence of retrogradely labelled perikarya in these structures is consistent with previous studies showing the existence of projections from the STN and GPe to the GPi.[7,8,11,30,34,38,45,49,57,67,68] However, the occurrence of labelled varicosities could not be explained by the anterograde transport of BDA from the GPi to the STN and GPe as these projections are thought to be very sparse[19,30] if they exist at all.[11,15,33] The most likely explanation for this labelling is that following injections of BDA in the GPi, the tracer was transported retrogradely to STN and GPe neurons, and then anterogradely, via axon collaterals, to terminal fields in the GPe and STN, respectively (Fig. 12A). Thus, we propose that most of the labelled terminals in the STN are derived from neurons in the GPe which retrogradely transported the BDA that was delivered in the GPi, and then antero-

gradely transported it to their terminals in the STN. Similarly, we propose that the labelled boutons in the GPe are derived from neurons in the STN which retrogradely transported the BDA that was injected in the GPi, and then anterogradely transported it to their terminals in the GPe (Fig. 12A). The fact that BDA can be transported in the retrograde direction to perikarya and then anterogradely along axon collaterals has been reported previously,[53] and indeed, we and others have observed this phenomenon with this and other tracers in the basal ganglia and the cerebral cortex.[6-8,35,67,68] Two approaches were taken to test these proposals. Firstly, we determined the ultrastructural features and neurotransmitter content of the labelled boutons in the STN and GPe. Secondly, we made injections of anterograde tracers in regions of the GPe corresponding to those regions that contained retrogradely labelled cells after injections in the GPi.

The electron microscopic analysis of the terminals labelled in the STN following tracer deposits in the GPi, revealed that the majority of boutons (type 1 terminals) were large, contained numerous mitochondria and pleomorphic vesicles that congregated at the active zone, formed symmetric synapses and displayed GABA immunoreactivity. These ultrastructural and neurochemical features are characteristic of those described in numerous studies of terminals arising from the GPe in monkeys[57,67,68] or the globus pallidus in rats.[8,58-61,73] The type 1 terminals are thus likely to be the terminals of neurons in the GPe and to have become labelled by the retrograde transport from the GPi to the GPe and then anterograde transport along long collaterals to the STN (Fig. 12A). The electron microscopic analysis of the terminals labelled in the GPe following tracer injection in the GPi revealed that in this case, the majority of terminals were medium sized, contained round synaptic vesicles, formed asymmetric synapses with dendritic shafts and were not immunoreactive for GABA. These features are characteristic of those described previously for terminals arising from neurons in the STN of monkeys[57,67,68] and rats.[6,7,38,55] It is therefore likely that these terminals are derived from neurons in the STN and were labelled by the retrograde transport of the marker and subsequent anterograde transport along collaterals (Fig. 12A).

In the second approach the assumption was made that, if the retrogradely labelled cells in the GPe are the source of labelled boutons in the STN, then injections of neuronal tracers in regions of retrograde labelling in the GPe should lead to anterograde labelling in the same part of the STN (Fig. 12B). The

Fig. 7. Schematic drawing through the globus pallidus (A–F) and STN (G–J) of the squirrel monkey to illustrate the distribution of labelled fibres (sinuous lines) and terminals (small black dots) after PHA-L injection in the ventral part of GPe (C). Note that the location of the injection site corresponds to that where the retrogradely labelled cells were found after injection in the ventrolateral region of GPi (see Fig. 5C). The anteroposterior coordinates are indicated in parentheses for each drawing.

A (A 12,5)

B (A 11,5)

C (A 11,0)

D (A 10,5)

E (A 10,0)

F (A 9,0)

G (A 8,5)   **H** (A 8,0)   **I** (A 7,5)   **J** (A 7,0)
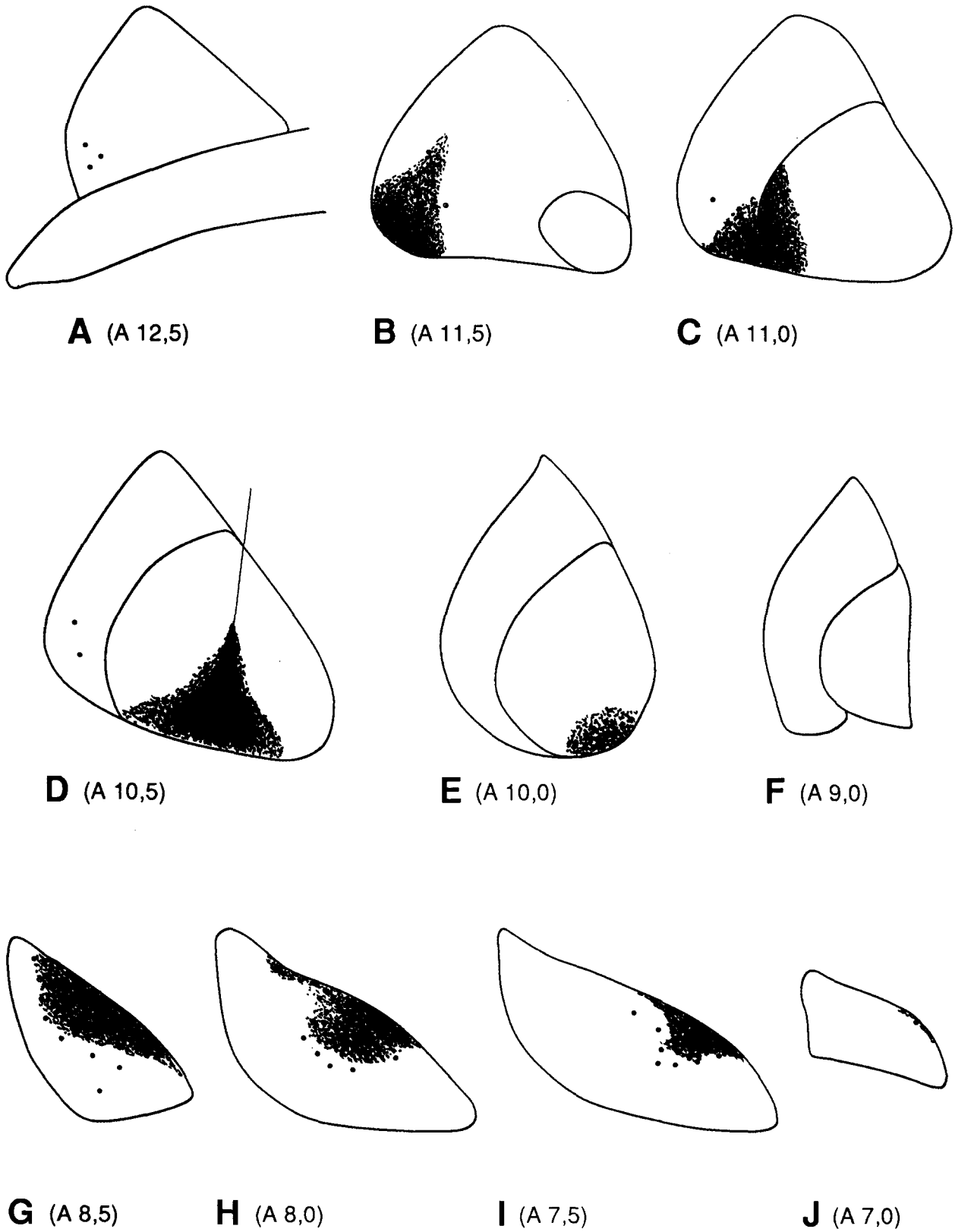
Fig. 8. Schematic drawing through the globus pallidus (A–F) and the STN (G–J) of the squirrel monkey to illustrate the distribution of labelled fibres (sinuous lines), terminals (small black dots) and perikarya (red dots) after BDA injection in the ventromedial region of GPi (D). One red dot indicates three retrogradely labelled cells. The anteroposterior coordinates are indicated in parentheses for each drawing.

results of this part of the study indicate that this is indeed the case. Thus, the deposits of BDA or PHA-L in regions of the GPe that contained retrogradely labelled cells after the GPi injections, led to clusters of labelled terminals in regions of the STN that corresponded closely to those labelled after injections in the GPi (compare Figs 1C and 1D; 2C and 2D). As one would predict, the deposits of tracer in the GPe also led to rich plexuses of labelled terminals in the regions of the GPi that had received the injections
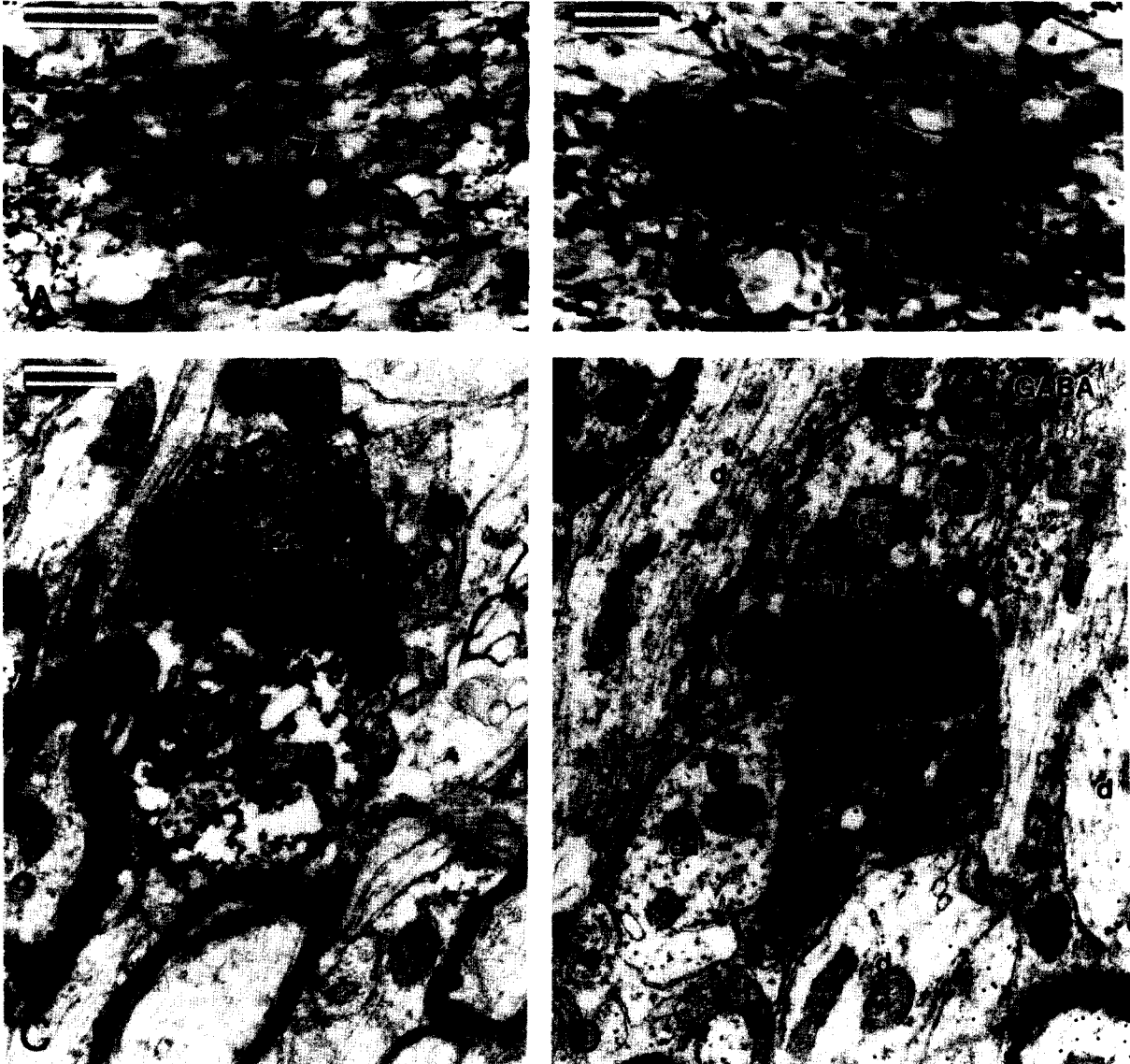
Fig. 9. Photomicrographs (A,B) and electron micrographs (C,D) showing various features of labelled structures in the STN after BDA injections in the ventrolateral part of the GPi. The micrographs in A and B were taken from the cluster of labelling shown in Fig. 2C. Note that BDA-labelled varicosities are apposed to the surface of both labelled (arrowheads in B) and unlabelled perikarya (arrowhead in A). The arrows in A indicate retrogradely labelled cells that are not contacted by BDA-positive terminals. (C,D) The two types of terminals visualized in the STN after BDA injections in the GPi. (C) A type 2 terminal that forms an asymmetric synapse (arrowheads) with a BDA-labelled dendritic shaft (d/BDA). The type 2 terminals accounted for 11% of the labelled boutons in the STN after BDA injections in the GPi. (D) Illustrates an example of a type 1 terminal that represents 89% of the total number of labelled boutons seen in the STN. The labelled terminal forms a symmetric synapse (arrows) with a dendritic shaft (d1). In a section that has been processed for the post-embedding immunohistochemical localization of GABA, the BDA-containing terminal is associated with a large number of gold particles which indicates that it displays GABA immunoreactivity (indicated by G). Another terminal in the same section (G1) is also immunoreactive for GABA whereas the bouton indicated by "G-" does not display immunoreactivity. The dendritic shafts (d) in the neuropil are non-immunoreactive for GABA. Scale bars = 100 μm (A); 20 μm (B); 0.5 μm (C, also applies to D).
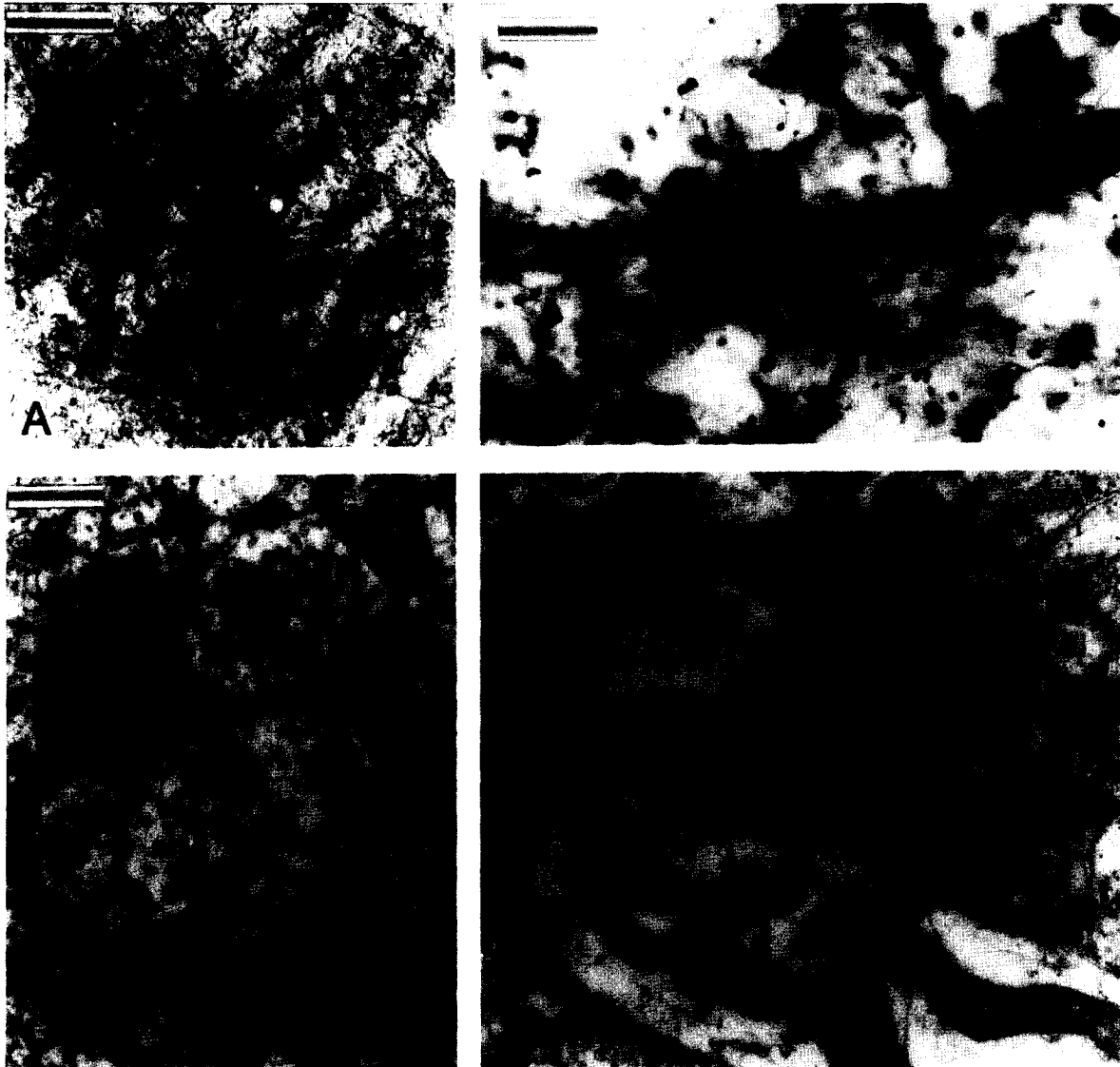
Fig. 10. Photomicrographs (A,B) and electron micrographs (C,D) showing various features of labelling in the GPe after injection of BDA in the ventrolateral two-thirds of the GPi (see Fig. 2A,E). (A) Shows a higher power view of the cluster of retrogradely labelled cells in register with BDA-containing varicosities indicated by an arrow in Fig. 2E. (B) Example of a retrogradely labelled cell in the core of the cluster of labelling in the GPe. The dendritic shaft of the labelled cell is apposed by numerous BDA-containing varicosities. (C) Examples of BDA-containing type 3 terminals apposed to the surface of a dendritic shaft (d). This type of terminal represents the least frequent population (7%) of labelled boutons encountered in the GPe after BDA injections in the GPi. These boutons display the ultrastructural features of striatal terminals and are immunoreactive for GABA. Note that the density of gold particles associated with these terminals is significantly higher than that overlying another bouton (indicated by "G-") in the neuropil. (D) An example of a BDA-labelled type 2 terminal that forms an asymmetric synapse (arrowhead) with a dendritic shaft (d). This type of terminal accounts for 82% of the labelled boutons found in the GPe after BDA injections in the GPi. In a GABA-immunostained section, these terminals are devoid of gold particles, which indicates that they are non-immunoreactive for GABA ("G-"). Note that other terminals in the neuropil are strongly immunoreactive for GABA ("G"). Scale bars = 0.25 mm (A); 20 μm (B); 0.5 μm (C, also applies to D).

of BDA (compare Fig. 1A and 1F). Electron-microscopic analysis of these terminals revealed two major populations. One type possessed the characteristics of terminals derived from the globus pallidus and were presumably labelled by the anterograde transport of the tracer from the GPe to the GPi. The second class displayed the ultrastructural features of terminals derived from the STN; which implies that they were presumably labelled by retrograde transport of tracer from the GPe to the STN and then anterograde transport to collaterals in the GPi. This phenomenon has also been observed in the entopeduncular nucleus

following tracer deposits in the globus pallidus of rats.[8]

These findings, together with previous data obtained with other neuronal tracers in the basal ganglia and other brain regions (see above), lead us to conclude therefore, that the axons and terminals that become labelled in the STN after injections of BDA in the GPi are the collaterals of GPe neurons that retrogradely transported the tracer and then distributed it throughout their axonal fields (Fig. 12A). Similarly, we conclude that the terminals labelled in the GPe after the tracer deposits in the GPi are derived from neurons in the STN that retrogradely transported the tracer to their somata and then anterogradely transported it, via long collaterals, to the GPe (Fig. 12A). Although the transport of BDA along the axon collaterals of retrogradely labelled cells could make the interpretation of the data obtained with this tracer difficult, our findings demonstrate that BDA also offers unique possibilities for studying the relationships between interconnected brain structures such as the pallidal complex and the STN. However, a prerequisite for such an application of BDA is a thorough knowledge of (i) the basic circuitry of the neuronal network under investigation, and (ii) the ultrastructural features and neurotransmitter content of the labelled terminals.

It should be noted that, in addition to the main population of terminals in both the STN and GPe that were labelled following tracer deposits in the GPi, a small proportion of labelled terminals in each structure displayed ultrastructural features different from the major group of labelled boutons. In the STN, a few labelled terminals (type 2 boutons) contained round synaptic vesicles and formed asymmetric axodendritic synapses. Based on these ultrastructural features, it is likely that these terminals arose from intrinsic axon collaterals of retrogradely labelled STN neurons, the existence of which has been previously demonstrated in the rat.[37] In the GPe, some labelled terminals displayed the ultrastructural features of pallidal boutons (type 1 terminals). This population of boutons may have been anterogradely labelled from the GPi[19,30] or may arise from intrinsic axon collaterals of retrogradely labelled GPe neurons.[39,67,68] A very small proportion of the labelled terminals in the GPe (type 3 boutons) contained ovoid synaptic vesicles, formed symmetric synapses and displayed GABA immunoreactivity. These characteristics are typical of those described on many occasions for the boutons of striatal projection neurons.[6-8,12,57,60] Since it is known that a proportion of neurons in the striatum project to the GPi and send axon collaterals to the GPe,[20,32,50] it is likely that the third type of terminals became labelled by retrograde transport from the GPi and then anterograde transport, via axon collaterals, to the GPe.

Neuronal network interconnecting the external pallidum and subthalamic nucleus with the internal pallidum

The present findings demonstrate a highly ordered and specific relationship between neurons of the pallidal complex and neurons in the STN. The specificity of the relationship is depicted by the close overlap between fields of terminals and retrogradely labelled cells in the STN and GPe after injections of tracers in the GPi. Thus, BDA injections in the GPi led to retrograde labelling of populations of neurons in both the GPe and STN that were embedded in dense networks of terminals derived from the STN and GPe, respectively. This reciprocity also occurred at the synaptic level. Many of the neurons in the STN that were retrogradely labelled from the GPi received synaptic input from terminals that were the collaterals of pallidal neurons that innervated the same region of the GPi. Similarly, neurons in the GPe that were retrogradely labelled from the GPi received synaptic input from the axon collaterals of subthalamic neurons that innervated the common region of the GPi.

The deposits of neuronal tracers in different regions of the internal and external segments of the globus pallidus and the subsequent anterograde and retrograde labelling that we observed demonstrate that the organizational principle of this neuronal network holds true for different functional regions of the GPe, STN and GPi. Our data thus confirm and extend previous findings relating to the topographical organization of the subthalamopallidal and the pallidosubthalamic projections in primates[11,45,62] and demonstrate that the functional specificity is maintained throughout the pallido-subthalamo-pallidal system. Thus, populations of neurons within sensorimotor, cognitive and limbic territories in the GPe are reciprocally connected with populations of neurons in the same functional territories of the STN and the neurons in each of these regions then, in turn, innervate the same functional territory of the GPi.[1,2,25,26,63,74,75]

An additional interesting and important conclusion of the present study is that neurons in the STN possess axon collaterals that innervate both segments of the pallidal complex. Although previous retrograde labelling studies in monkeys have suggested that projections to the GPe or GPi largely arise from different populations of neurons in the STN,[11,50] these conclusions were based on the analysis of retrograde labelling in the STN after large injections of horseradish peroxidase[11] or fluorescent dyes[50] in one or the other pallidal segment. The fact that these injections were large and, as is now apparent, did not involve interconnected regions of the GPe and GPi may explain the discrepancy between our findings and those obtained in these studies. However, our data do not necessarily indicate that all STN neurons project to both pallidal segments. After BDA
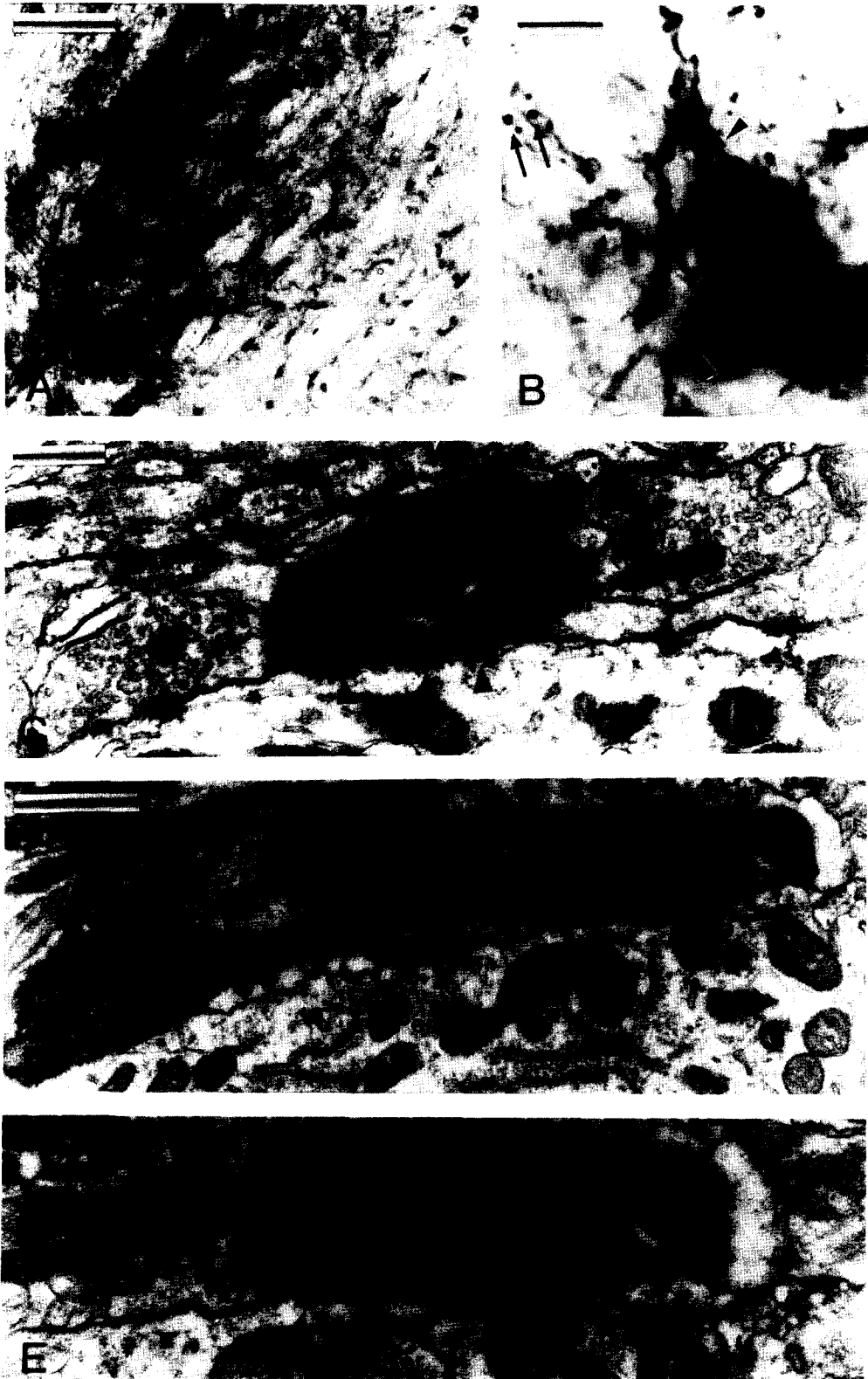
Fig. 11.
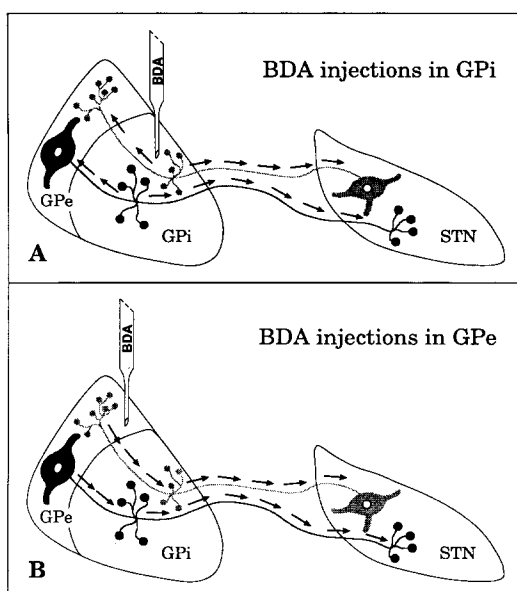
Fig. 12. Schematic diagrams that show the possible sources of labelling in the pallidal complex and the STN following injections of BDA in the GPi (A) or GPe (B). The arrows indicate the directions that the tracer is expected to have been transported to produce the observed results. (A) After injections in GPi, BDA is transported retrogradely to GPe and STN and then anterogradely, via axon collaterals, to the STN and GPe respectively. (B) After injections in the GPe, BDA is transported retrogradely to the STN and then anterogradely, via axon collaterals, to the GPi. BDA is also transported anterogradely to the GPi and STN.

Fig. 13. Schematic diagram to summarize the relationships between the two pallidal segments and the STN such as revealed in the present study. Small groups of interconnected neurons in the associative (A) and sensorimotor (B) territories of GPe and STN innervate, via axon collaterals, a common functionally-related region in the GPi.

injections in either segment of the globus pallidus, a significant number of cells in register with the field of labelled terminals remained unlabelled in the STN. Although the projection site of these neurons was not determined, a possibility could be that these cells innervate exclusively the segment of the globus pallidus that was not injected with BDA. Of course, an alternative explanation is that these neurons project to other targets of the STN including the substantia nigra[45,49,62,63] or the pedunculopontine nucleus.[49] Intracellular filling of single STN neurons will resolve this issue. Similar findings were obtained in the GPe after BDA injections in the GPi. The fact that some GPe cells remained unlabelled in the core of the terminal field after injections in the GPi (see Fig. 4C)

may indicate that not all GPe neurons project to both GPi and STN. These data are in keeping with those obtained in a recent intracellular study in the rat.[39]

The organizational principle that we describe is not consistent with the current view (see Introduction) that the STN provides a widespread, "nonspecific" excitatory influence on the globus pallidus, rather, neurons in the STN are in a position to produce a very specific excitatory effect on small populations of related neurons in the GPe and GPi. It should be noted however, that following the deposits of tracer in the GPi occasional retrogradely labelled neurons were located outside of the region of axon and terminal labelling in the GPe and STN. It is unclear at present whether this observation simply reflects the fact that the tracer deposits extended in the dorsolateral plane, thus contaminating neighbouring functional regions or whether the tracer was taken up by distal segments of damaged axons that extend out of the injection site. Of course, another alternative is that the organizational principle that we have

Fig. 11. Photomicrographs (A,B) and electron micrographs (C–E) showing labelled elements in the GPi after injection of BDA in the dorsal third of the GPe (see Fig. 1B,F). (A) Higher power view of the aggregate of labelled varicosities indicated by an arrow in Fig. 1F. (B) Neuronal perikaryon in the core of the terminal field in the GPi. This cell body is tightly surrounded by large varicosities (arrowheads). Another population of terminal-like structures (indicated by arrows) occurs in the neuropil. (C) An example of a BDA-containing type 2 terminal that forms an asymmetric synapse (arrowheads) with a dendritic shaft. This population of boutons account for 50% of the labelled terminals seen in the GPi after BDA injections in the dorsal third of the GPe. (D,E) BDA-containing boutons that display the ultrastructural features of type 1 terminals and form symmetric synapses (arrows) with a perikaryon (per). Note in D that the two boutons arise from a single axon, as it was expected to be the case for the large-sized varicosities (arrowheads) apposed to the surface of the perikaryon in B. Forty-four per cent of the total number of labelled boutons in the GPi after BDA injections in the GPe belong to the population of type 1 terminals. Scale bars = 0.25 mm (A); 20 μm (B); 0.5 μm (C, also applies to E); 1 μm (D).

identified overlies an additional, albeit less promi-
nent, system in which there is not a correspondence
between functionally related neurons. The only way
to fully solve this issue is to fill intracellularly single
STN cells and trace their full axonal arborization in
the GPe and GPi. However, because of the location
and size of the STN, intracellular filling of cells in this
nucleus is a very difficult task in the monkey brain.

Functional considerations

The new organizational principle of the intercon-
nections between the GPe, STN and GPi that we have
described has important implications for the under-
standing of the neuronal mechanisms by which the
so-called indirect pathways[2,14] are involved in the
control of motor commands in primates and the
interpretation of electrophysiological data. Firstly, it
is clear that axons of subthalamic neurons are not
widely spread in the GPe or GPi. In contrast, specific
groups of functionally related STN neurons send
projections that terminate with a high degree of
specificity in restricted regions of the GPe and GPi.
Thus, in the analysis of synaptic interactions between
neurons in the pallidal complex and STN it is critical
to select the interconnected functionally related re-
gions of each structure. The failure to detect synchro-
nization between pairs of STN and pallidal neurons
in electrophysiological analyses in primates[4] may
simply reflect the failure to locate interconnected
neurons rather than a diffuse connection between the
STN and the pallidum. In keeping with this possi-
bility, recent data showed that the activity of pallidal
neurons in normal monkeys is non-synchronized,
which indicates that the spiking activity of pallidal
cells is not driven by common inputs.[46] Secondly, the
network that we describe provides an anatomical
substrate for the complex excitatory and inhibitory
responses that occur in output neurons of the basal
ganglia following activation of the indirect pathway.[21]
Thus, although it is evident that a major excitatory
"driving force" of GPi cells are neurons in the
STN,[3,5,18,27,36,41,76] it is likely that the same pool of
neurons in the STN inhibit indirectly, the same

neurons in the GPi by activation of the neurons in the
GPe that project to the common region of the GPi.
The neuronal mechanisms by which the opposite
effects generated by activation of the STN–GPi and
the STN–GPe–GPi projections are integrated at the
level of single GPi cells remains to be established. The
complex pattern of increased and decreased activity
of the basal ganglia output neurons during a motor
act[10,22,42,44] probably relies on precise temporal inter-
actions between the activities of the inhibitory GPe
and striatal afferents with that of the excitatory
subthalamic input to single GPi neurons. Future
electrophysiological data relating to the activity of
interconnected pairs of GPe and GPi neurons follow-
ing stimulation of the STN are essential to further our
understanding of these issues.

CONCLUSIONS

The results of our study raise several important
issues concerning the circuitry connecting the two
pallidal segments and the subthalamic nucleus as well
as the mechanisms by which information is processed
in the basal ganglia. Firstly, the connections between
the two segments of the pallidum and the STN show
a high degree of specificity such that small groups of
neurons in the GPe and STN innervate common
regions in the GPi and are reciprocally connected at
the synaptic level. Secondly, the topographical distri-
bution of the interconnected neurons respects the
known functional organization of the two segments
of the globus pallidus and the STN. Thirdly, the
findings imply that individual neurons in the GPe
project via collaterals to both the GPi and STN and,
similarly, that neurons in the STN project to both the
GPi and GPe.

REFERENCES

1. Alexander G. E., DeLong M. R. and Strick P. L. (1986) Parallel organization of functionally segregated circuits linking basal ganglia and cortex. *A. Rev. Neurosci.* **9**, 357–381.
2. Alexander G. E. and Crutcher M. D. (1990) Functional architecture of basal ganglia circuits: neural substrates of parallel processing. *Trends Neurosci.* **13**, 266–271.
3. Aziz T. Z., Peggs D., Sambrook M. A. and Crossman A. R. (1991) Lesion of the subthalamic nucleus for the alleviation of 1-methyl-4-phenyl-1,2,3,6-tetrahydropyridine (MPTP)-induced Parkinsonism in the primate. *Mov. Disorders* **6**, 288–292.
4. Bergman H. and DeLong M. R. (1989) Electro-physiological studies of the connections of the subthalamic nucleus and globus pallidus in behaving monkeys. *Soc. Neurosci.* **15**, 902.
5. Bergman H., Wichmann T. and DeLong M. R. (1990) Reversal of experimental parkinsonism by lesions of the subthalamic nucleus. *Science* **249**, 1436–1438.
6. Bevan M. D., Bolam J. P. and Crossman A. R. (1994) Convergent synaptic input from the neostriatum and the subthalamus onto identified nigrothalamic neurons in the rat. *Eur. J. Neurosci.* **6**, 320–334.
7. Bevan M. D., Crossman A. R. and Bolam J. P. (1994) Neurons projecting from the entopeduncular nucleus to the thalamus receive convergent synaptic inputs from the subthalamic nucleus and the neostriatum in the rat. *Brain Res.* **659**, 99–109.

8. Bolam J. P. and Smith Y. (1992) The striatum and the globus pallidus send convergent synaptic inputs onto single cells in the entopeduncular nucleus of the rat: a double anterograde labelling study combined with post-embedding immunocytochemistry for GABA. *J. comp. Neurol.* **321**, 456–476.

9. Brandt H. M. and Apkarian A. V. (1992) Biotin-dextran: a sensitive anterograde tracer for neuroanatomic studies in rat and monkey. *J. Neurosci. Meth.* **45**, 35–40.

10. Brotchie P., Iansek R. and Horne M. K. (1991) Motor function of the monkey globus pallidus. 1. Neuronal discharge and parameters of movement. *Brain* **114**, 1667–1683.

11. Carpenter M. B., Batton R. R. III, Carleton S. C. and Keller J. T. (1981) Interconnections and organization of pallidal and subthalamic nucleus neurons in the monkey. *J. comp. Neurol.* **197**, 579–603.

12. Chang H. T., Wilson C. J. and Kitai S. T. (1981) Single neostriatal efferent axons to the globus pallidus: a light and electron microscopic study. *Science* **213**, 915–918.

13. Dale N., Ottersen O. P., Roberts A. and Storm-Mathisen J. (1986) Inhibitory neurones of a motor pattern generator in *Xenopus* revealed by antibodies to glycine. *Nature* **324**, 255–257.

14. DeLong M. R. (1990) Primate models of movement disorders of basal ganglia origin. *Trends Neurosci.* **13**, 281–285.

15. DeVito J. L. and Anderson M. E. (1982) An autoradiographic study of efferent connections of the globus pallidus in *Macaca mulatta*. *Expl Brain Res.* **46**, 107–117.

16. DeVito J. L., Anderson M. E. and Walsh K. E. (1980) A horseradish peroxidase study of afferent connections of the globus pallidus in *Macaca mulatta*. *Expl Brain Res.* **38**, 65–73.

17. Emmers R. and Akert K. (1963) *A Stereotaxic Atlas of the Brain of the Squirrel Monkey* (Saimiri sciureus). University of Wisconsin Press, Madison.

18. Féger J. and Robledo P. (1991) The effects of activation or inhibition of the subthalamic nucleus on the metabolic and electrophysiological activities within the pallidal complex and substantia nigra in the rat. *Eur. J. Neurosci.* **3**, 947–952.

19. Fink-Jensen A. and Mikkelsen J. D. (1991) A direct projection from the entopeduncular nucleus to the globus pallidus. A PHA-L anterograde tracing study in the rat. *Brain Res.* **542**, 175–179.

20. Flaherty A. W. and Graybiel A. M. (1993) Output architecture of the primate putamen. *J. Neurosci.* **13**, 3222–3237.

21. Fujimoto K. and Kita H. (1992) Responses of rat substantia nigra pars reticulata units to cortical stimulation. *Neurosci. Lett.* **142**, 105–109.

22. Georgopoulos A. P., DeLong M. R. and Crutcher M. D. (1983) Relations between parameters of step-tracking movements and single cell discharge in the globus pallidus and subthalamic nucleus of the behaving monkey. *J. Neurosci.* **3**, 1586–1598.

23. Gerfen C. R. (1985) The neostriatal mosaic: I. Compartmental organization of projections from the striatum to the substantia nigra in the rat. *J. comp. Neurol.* **236**, 454–476.

24. Gerfen C. R. and Sawchenko P. E. (1984) An anterograde neuroanatomical tracing method that shows the detailed morphology of neurons, their axons and terminals: immunohistochemical localization of an axonally transported plant lectin, *Phaseolus vulgaris*-leucoagglutinin (PHA-L). *Brain Res.* **290**, 219–238.

25. Groenewegen H. J., Berendse H. W. and Haber S. N. (1993) Organization of the output of the ventral striatopallidal system in the rat: ventral pallidal efferents. *Neuroscience* **57**, 113–142.

26. Haber S. N., Lyn-Balta E. and Mitchell S. J. (1993) The organization of the descending ventral pallidal projections in the monkey. *J. comp. Neurol.* **329**, 111–128.

27. Hamada I. and DeLong M. R. (1992) Excitotoxic acid lesions of the primate subthalamic nucleus result in reduced pallidal neuronal activity during active holding. *J. Neurophysiol.* **68**, 1859–1866.

28. Hazrati L.-N. and Parent A. (1992) The striatopallidal projection displays a high degree of anatomical specificity in the primate. *Brain Res.* **592**, 213–227.

29. Hazrati L.-N. and Parent A. (1992) Convergence of subthalamic and striatal efferents at pallidal level in primates: an anterograde double-labeling study with biocytin and PHA-L. *Brain Res.* **569**, 336–340.

30. Hazrati L.-N., Parent A., Mitchell S. and Haber S. N. (1990) Evidence for interconnections between the two segments of the globus pallidus in primates: a PHA-L anterograde tracing study. *Brain Res.* **533**, 171–175.

31. Hodgson A. J., Penke B., Erdei A., Chubb I. W. and Somogyi P. (1985) Antisera to γ-aminobutyric acid. I. Production and characterization using a new model system. *J. Histochem. Cytochem.* **33**, 229–239.

32. Kawaguchi Y., Wilson C. J. and Emson P. C. (1990) Projection subtypes of rat neostriatal matrix cells revealed by intracellular injection of biocytin. *J. Neurosci.* **10**, 3421–3438.

33. Kim R., Nakano K., Jayaraman A. and Carpenter M. B. (1976) Projections of the globus pallidus and adjacent structures: an autoradiographic study in the moneky. *J. comp. Neurol.* **169**, 263–290.

34. Kincaid A. E., Newman S. W., Young A. B. and Penney J. B. (1990) Evidence for a projection from the globus pallidus to the entopeduncular nucleus in the rat. *Neurosci. Lett.* **128**, 121–125.

35. Kisvarday Z. F. and Eysel U. T. (1992) Cellular organization of reciprocal patchy networks in layer III of cat visual cortex (area 17). *Neuroscience* **46**, 275–286.

36. Kita H. (1993) Physiology of two disynaptic pathways from the sensorimotor cortex to the basal ganglia output nuclei. In *The Basal Ganglia IV—New Ideas and Data on Structure and Function* (eds Percheron G., McKenzie J. S. and Féger J.), pp. 263–276. Plenum, New York.

37. Kita H., Chang H. T. and Kitai S. T. (1983) The morphology of intracellularly labeled rat subthalamic neurons: a light microscopic analysis. *J. comp. Neurol.* **215**, 245–257.

38. Kita H. and Kitai S. T. (1987) Efferent projections of the subthalamic nucleus in the rat: light and electron microscopic analysis with the PHA-L method. *J. comp. Neurol.* **260**, 435–452.

39. Kita H. and Kitai S. T. (1994) The morphology of globus pallidus projection neurons in the rat: an intracellular staining study. *Brain Res.* **636**, 308–319.

40. Kitai S. T. and Kita H. (1987) Dual striatonigral inhibitory actions. In *Proceedings of the International Conference Neural Mechanisms of Disorders of Movement*, p. 21. Manchester, U.K.

41. Kitai S. T. and Kita H. (1987) Anatomy and physiology of the subthalamic nucleus: a driving force of the basal ganglia. In *The Basal Ganglia II—Structure and Function: Current Concepts* (eds Carpenter M. B. and Jayaraman A.), pp. 357–373. Plenum, New York.

42. Mink J. W. and Thach W. T. (1991) Basal ganglia motor control. III. Pallidal ablation: normal reaction time, muscle cocontraction, and slow movement. *J. Neurophysiol.* **65**, 330–351.

43. Mink J. W. and Thach W. T. (1993) Basal ganglia intrinsic circuits and their role in behavior. *Curr. Opin. Neurobiol.* **3**, 950–957.

44. Mitchell S. J., Richardson R. T., Baker F. H. and DeLong M. R. (1987) The primate globus pallidus: neuronal activity related to direction of movement. *Expl Brain Res.* **68**, 491–505.

45. Nauta H. J. W. and Cole M. (1978) Efferent projections of the subthalamic nucleus: an autoradiographic study in monkey and cat. *J. comp. Neurol.* **180**, 1–16.

46 Nini A., Feingold A., Slovin H. and Bergman H. (1995) Neurons in the globus pallidus do not show correlated activity in the normal monkey, but phase-locked oscillations appear in the MPTP model of parkinsonism. *J. Neurophysiol.* **74**, 1800–1805.

47. Parent A. (1990) Extrinsic connections of the basal ganglia. *Trends Neurosci.* **13**, 254–258.

48. Parent A. and Hazrati L.-N. (1993) Anatomical aspects of information processing in primate basal ganglia. *Trends Neurosci.* **16**, 111–116.

49. Parent A. and Smith Y. (1987) Organization of the efferent projections of the subthalamic nucleus in the squirrel monkey as revealed by retrograde labeling methods. *Brain Res.* **436**, 296–310.

50. Parent A., Smith Y., Filion M. and Dumas J. (1989) Distinct afferents to internal and external pallidal segments in the squirrel monkey. *Neurosci. Lett.* **96**, 140–144.

51. Phend K. D., Weinberg R. J. and Rustioni A. (1992) Techniques to optimize post-embedding single and double staining for amino acid neurotransmitters. *J. Histochem. Cytochem.* **40**, 1011–1020.

52. Rajakumar N., Elisevich K. and Flumerfelt B. A. (1993) Biotinylated dextran: a versatile anterograde and retrograde neuronal tracer. *Brain Res.* **607**, 47–53.

53. Reiner A., Veenman C. L. and Honig M. G. (1993) Anterograde tracing using biotinylated dextran amine. *Neurosci. Protocols* 93-050-14-01.

54. Reynolds E. S. (1963) The use of lead citrate at high pH as an electron opaque stain in electron microscopy. *J. Cell Biol.* **17**, 208–212.

55. Rinvik E. and Ottersen O. P. (1993) Terminals of subthalamonigral fibres are enriched with glutamate-like immunoreactivity: an electron microscopic, immunogold analysis in the cat. *J. chem. Neuroanat.* **6**, 19–30.

56. Rouzaire-Dubois B., Hammond C., Yelnik J. and Féger J. (1984) Anatomy and neurophysiology of subthalamic efferent neurons. In *The Basal Ganglia, Structure and Function* (eds Kemm R. E. and Wilcock L. N.), pp. 205–234. Plenum, New York.

57. Shink E. and Smith Y. (1995) Differential synaptic innervation of neurones in the internal and the external segments of the globus pallidus by the GABA- and glutamate-containing terminals in the squirrel monkey. *J. comp. Neurol.* **358**, 119–141.

58. Smith Y. and Bolam J. P. (1989) Neurons of the substantia nigra reticulata receive a dense GABA-containing input from the globus pallidus in the rat. *Brain Res.* **493**, 160–167.

59. Smith Y. and Bolam J. P. (1990) The output neurones and the dopaminergic neurones of the substantia nigra receive a GABA-containing input from the globus pallidus in the rat. *J. comp. Neurol.* **296**, 47–64.

60. Smith Y. and Bolam J. P. (1991) Convergence of synaptic inputs from the striatum and the globus pallidus onto identified nigrocollicular cells in the rat: a double anterograde labelling study. *Neuroscience* **44**, 45–73.

61. Smith Y., Bolam J. P. and von Krosigk M. (1990) Topographical and synaptic organization of the GABA-containing pallidosubthalamic projection in the rat. *Eur. J. Neurosci.* **2**, 500–511.

62. Smith Y., Hazrati L.-N. and Parent A. (1990) Efferent projections of the subthalamic nucleus in the squirrel monkey as studied by the PHA-L anterograde tracing method. *J. comp. Neurol.* **294**, 306–323.

63. Smith Y. and Parent A. (1986) Differential connections of caudate nucleus and putamen in the squirrel monkey (*Saimiri sciureus*). *Neuroscience* **18**, 347–371.

64. Smith Y., Parent A. and Dumas J. (1988) Organization of efferent connections of the two pallidal segments in primate as revealed by PHA-L anterograde tracing method. *Soc. Neurosci.* **14**, 719.

65. Smith Y., Shink E., Bevan M. D. and Bolam J. P. (1995) The subthalamic nucleus and the external pallidum: two tightly interconnected structures that control the output of the basal ganglia in primates. *Brain Res. Ass. Abstr.* **12**, 89.

66. Smith Y., Sidibé M. and Shink E. (1994) A light and electron microscopic analysis of the interconnections between the two pallidal segments and the subthalamic nucleus in the squirrel monkey. *Soc. Neurosci.* **20**, 332.

67. Smith Y., Wichmann T. and DeLong M. R. (1993) The external pallidum and the subthalamic nucleus send convergent synaptic inputs onto single neurones in the internal pallidal segment in monkey: anatomical organization and functional significance. In *The Basal Ganglia IV: New Ideas and Data on Structure and Function* (eds Percheron G., McKenzie J. S. and Féger J.), pp. 51–62. Plenum, New York.

68. Smith Y., Wichmann T. and DeLong M. R. (1994b) Synaptic innervation of neurones in the internal pallidal segment by the subthalamic nucleus and the external pallidum in monkeys. *J. comp. Neurol.* **343**, 297–318.

69. Somogyi P. and Hodgson A. J. (1985) Antisera to γ-aminobutyric acid. III. Demonstration of GABA in Golgi-impregnated neurons and in conventional electron microscopic sections of cat striate cortex. *J. Histochem. Cytochem.* **33**, 249–257.

70. Somogyi P., Hodgson A. J., Chubb I. W., Penke B. and Erdei A. (1985) Antisera to γ-aminobutyric acid. II. Immunocytochemical application to the central nervous system. *J. Histochem. Cytochem.* **33**, 240–248.

71. Staines W. A. (1988) PHA-L studies of the efferent connections of the rat globus pallidus. *Soc. Neurosci. Abstr.* **16**, 427.

72. Veenman C. L., Reiner A. and Honig M. G. (1992) Biotinylated dextran amine as an anterograde tracer for single- and double-labeling studies. *J. Neurosci. Meth.* **41**, 239–254.

73. Von Krosigk M., Smith Y., Bolam J. P. and Smith A. D. (1992) Synaptic organization of GABAergic inputs from the striatum and the globus pallidus onto neurons in the substantia nigra and retrorubral field which project to the medullary reticular formation. *Neuroscience* **50**, 531–549.

74. Von Monakow K. H., Akert K. and Künzle H. (1978) Projections of the precentral motor cortex and other cortical areas of the frontal lobe to the subthalamic nucleus in the monkey. *Expl Brain Res.* **33**, 395–403.

75. Wichmann T., Bergman H. and DeLong M. R. (1994) The primate subthalamic nucleus. I. Functional properties in intact animals. *J. Neurophysiol.* **72**, 494–506.
76. Wichmann T., Bergman H. and DeLong M. R. (1994) The primate subthalamic nucleus. III. Changes in motor behavior and neuronal activity in the internal pallidum induced by subthalamic inactivation in the MPTP model of Parkinsonism. *J. Neurophysiol.* **72**, 521–530.
77. Wilson C. J. and Phelan K. D. (1982) Dual topographic representation of neostriatum in the globus pallidus of rats. *Brain Res.* **243**, 354–359.